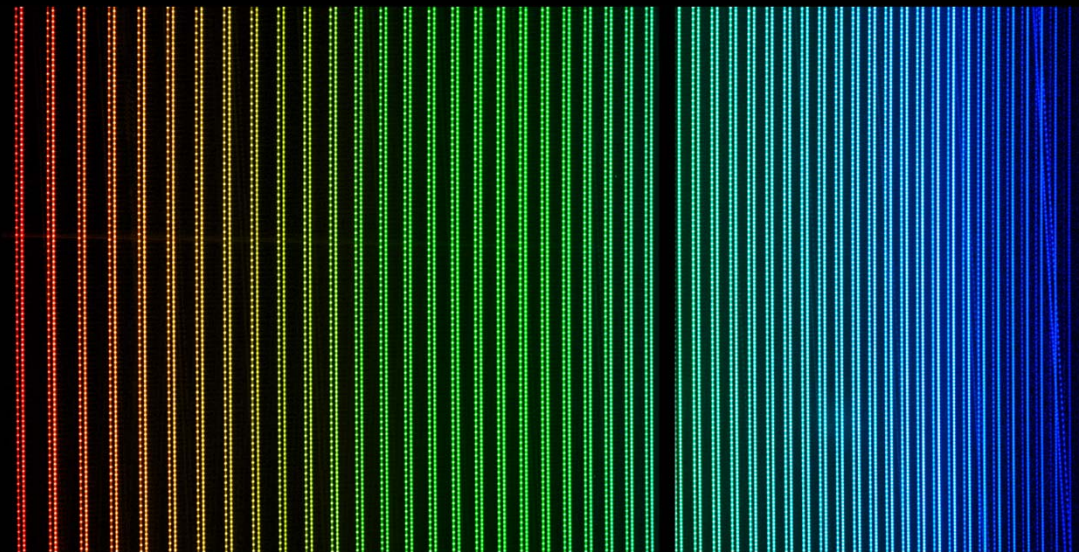


Fraunhofer's hand-colored map of the solar spectrum (ca. 1814; Deutsches Museum, München)



HARPS spectra of two laser frequency combs (ESO)

Spectral Fidelity

Opportunities, limitations, and future challenges

Dainis Dravins

Lund Observatory, Lund University, Sweden

www.astro.lu.se/~dainis



LUND
UNIVERSITY

PHILOSOPHY

THE QUEST FOR TRUTH



PHILOSOPHY

What limits accuracy?

What requires $S/N \gg 1000$?

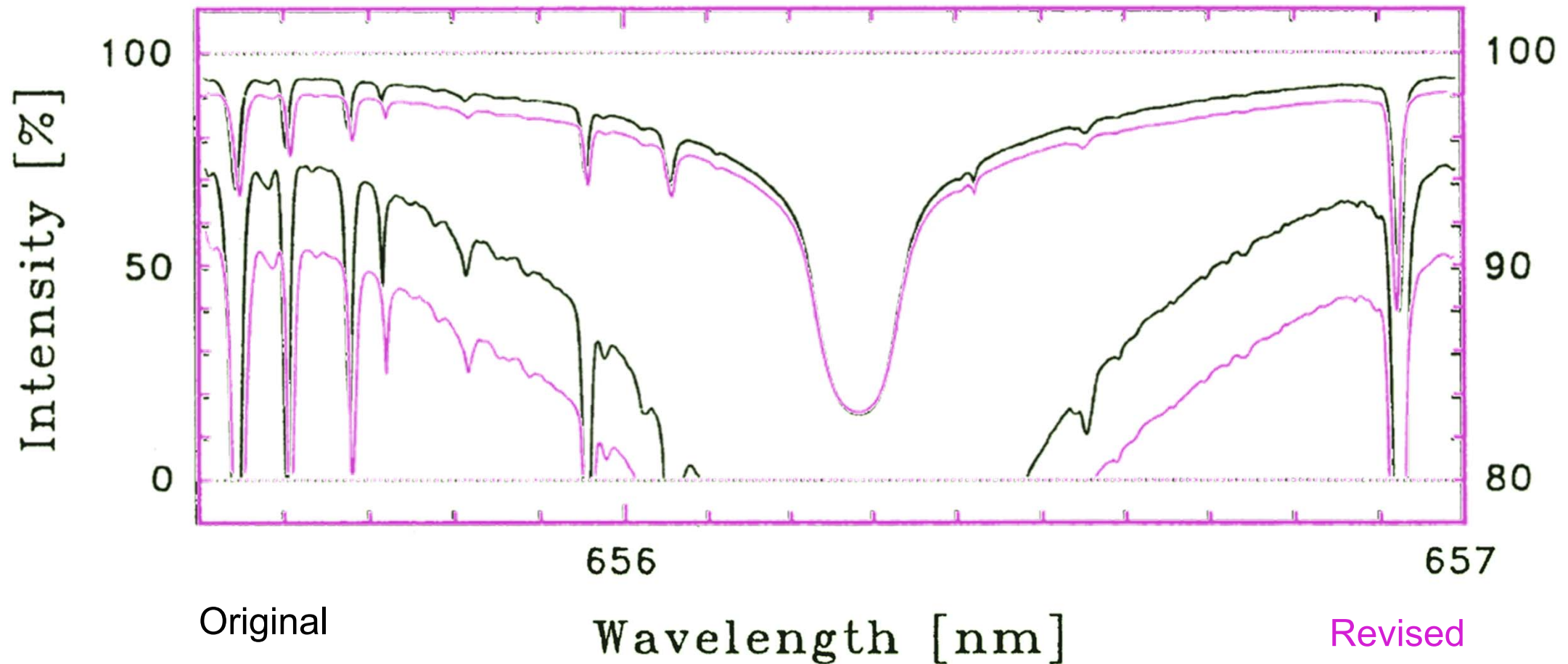
What requires $\lambda/\Delta\lambda = 1,000,000$?

What requires post-CCD detectors?

What can still not be measured?

**From precision
to accuracy**

Highest-precision atlases of the Solar spectrum



$$\lambda/\Delta\lambda \approx 10^6$$

S/N = 2000 or 20 ??

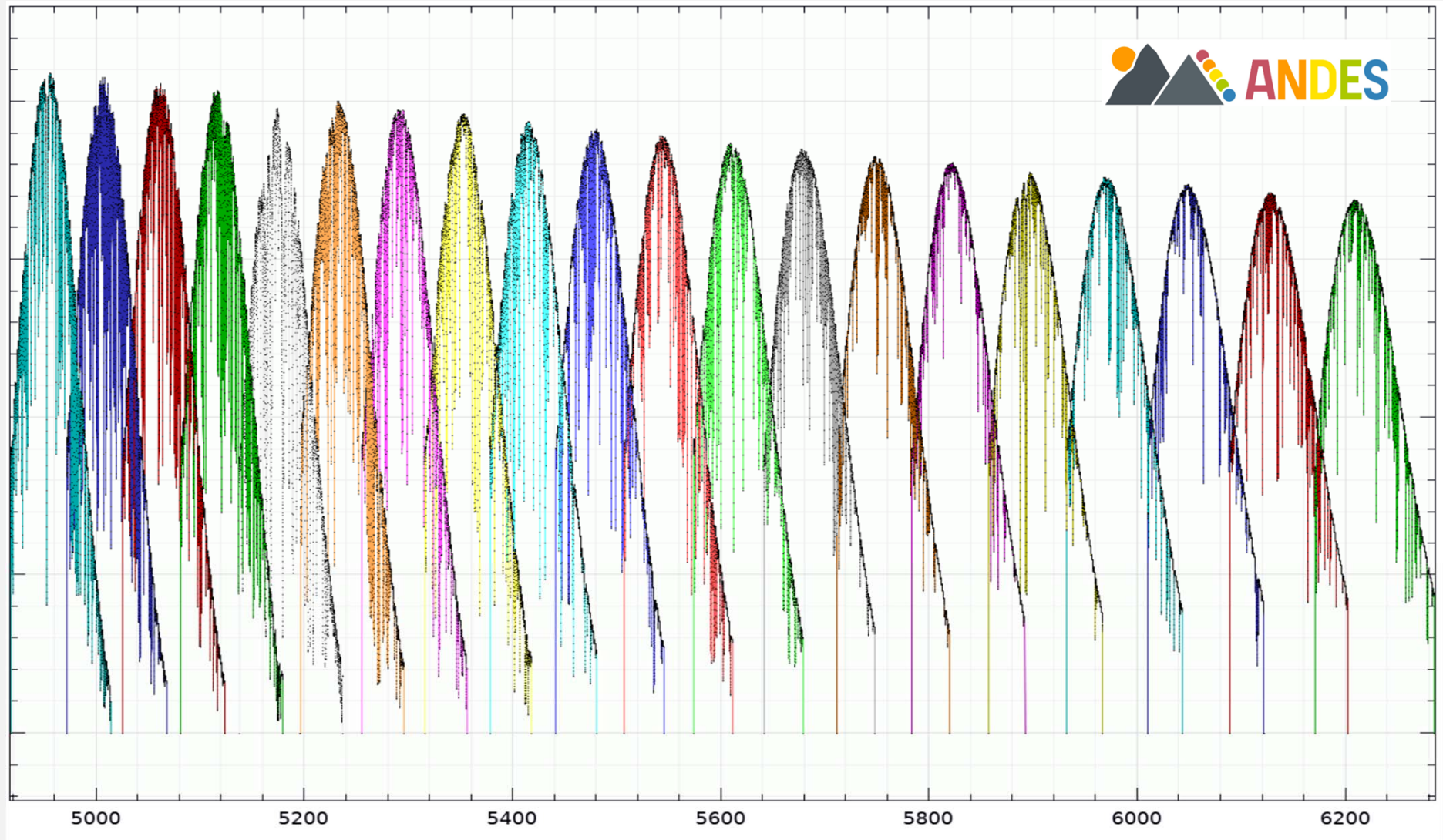
L.Delbouille, G.Roland, L.Neven

Atlas photométrique du spectre solaire de λ 3000 à λ 10000

Institut d'Astrophysique de l'Université de Liège, Observatoire Royal de Belgique, 1973-1988 – this revision 1979

**What is limiting
the fidelity ?**

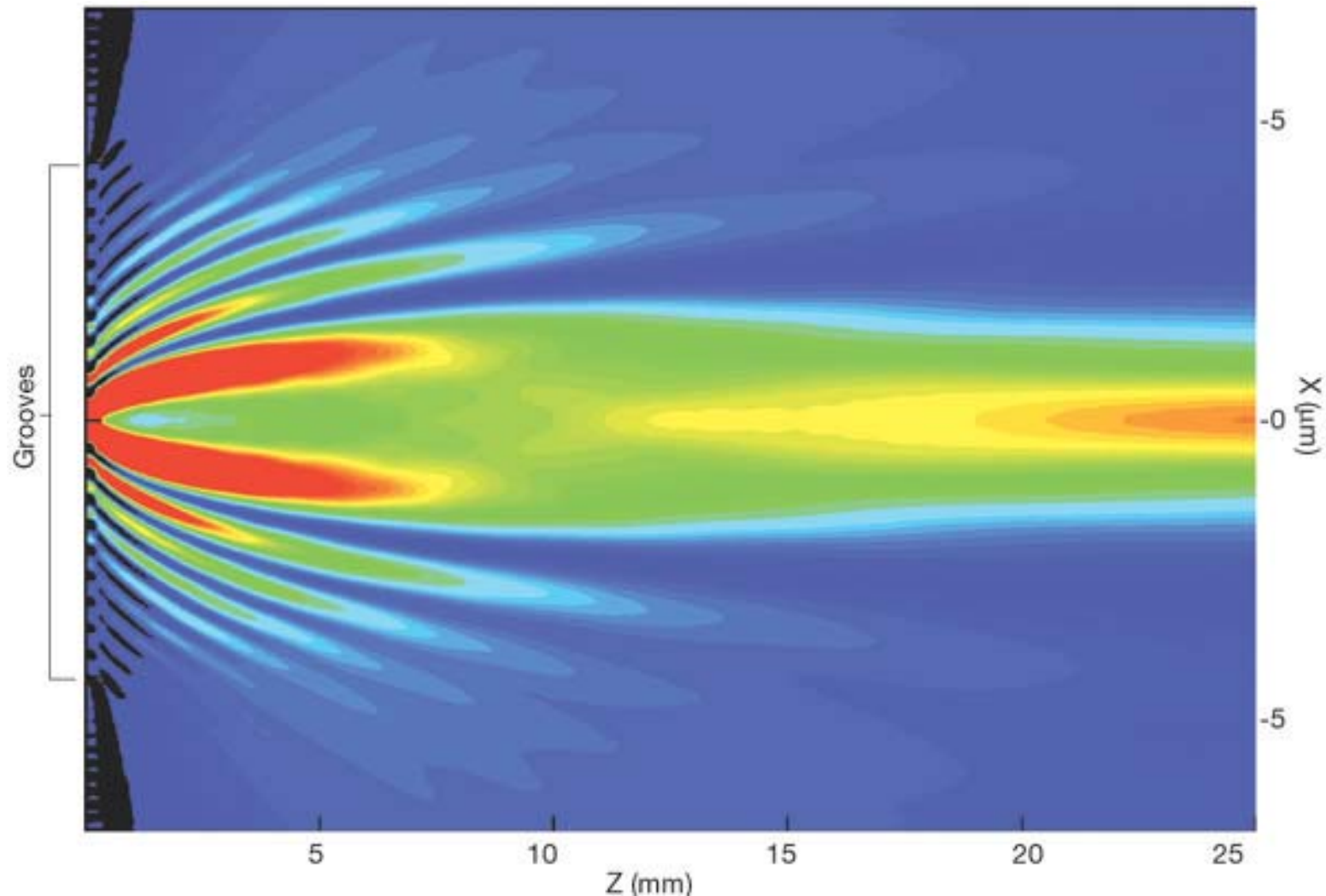
Continuum calibration issues



Simulated extracted solar spectrum from the ANDES spectrometer @ ELT

Michael Weber, Manfred Woche, Ilya Ilyin, Klaus G. Strassmeier, Ernesto Oliva:
ANDES, the high resolution spectrometer for the ELT: The UVB spectrograph module
Proc. SPIE **12184**, 1218439 (2022)

Grating physics is complex...

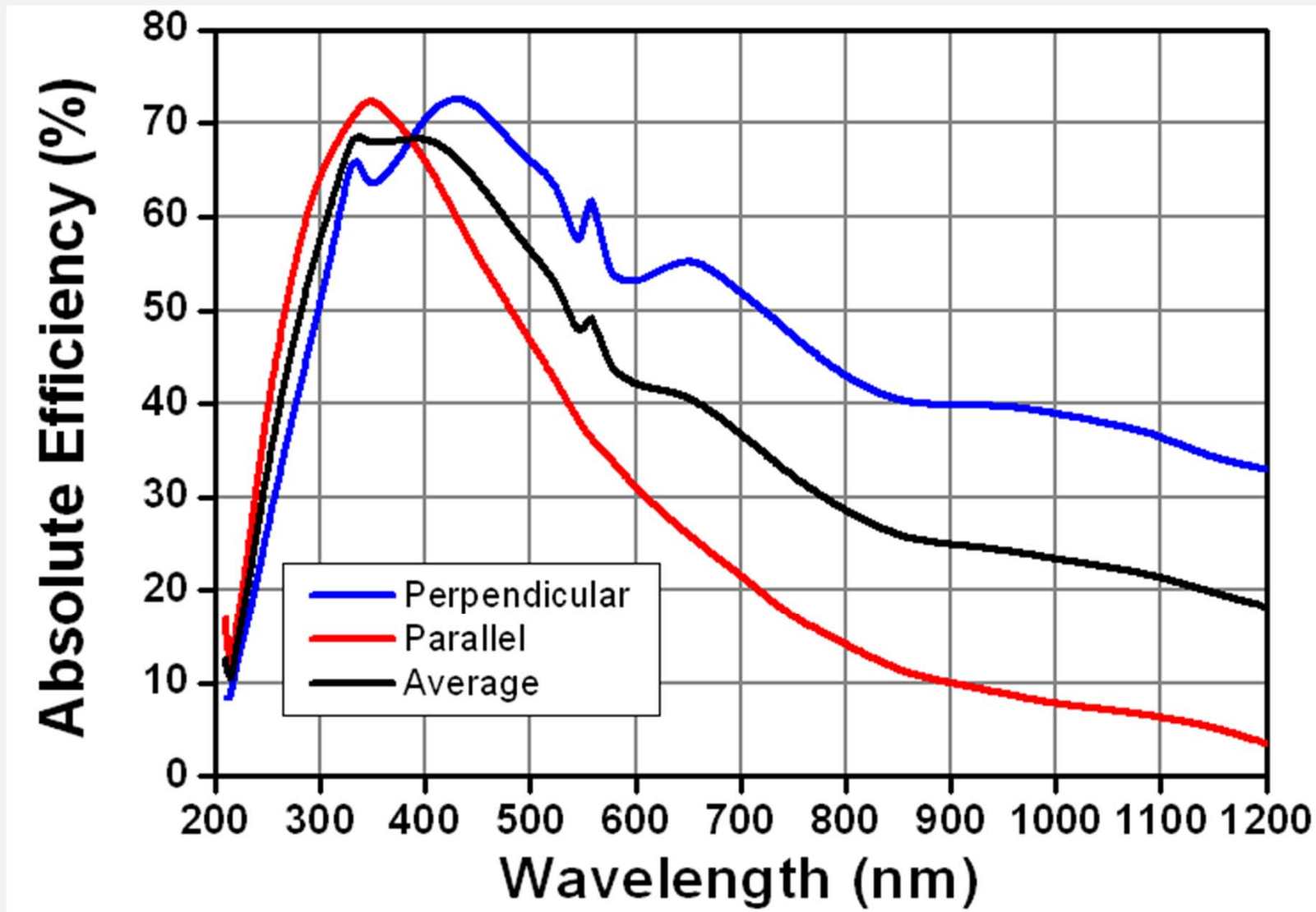


Calculated pattern of light emerging from a slit surrounded by an array of grooves

Simulation with 10 grooves on each side of the slit, each 40 nm wide and 100 nm deep, with period 500 nm. The plot shows the spatial dependence of the component of the Poynting vector along the radial direction for a wavelength of 560 nm (spectral transmission maximum). Blue denotes low intensity, and red high.

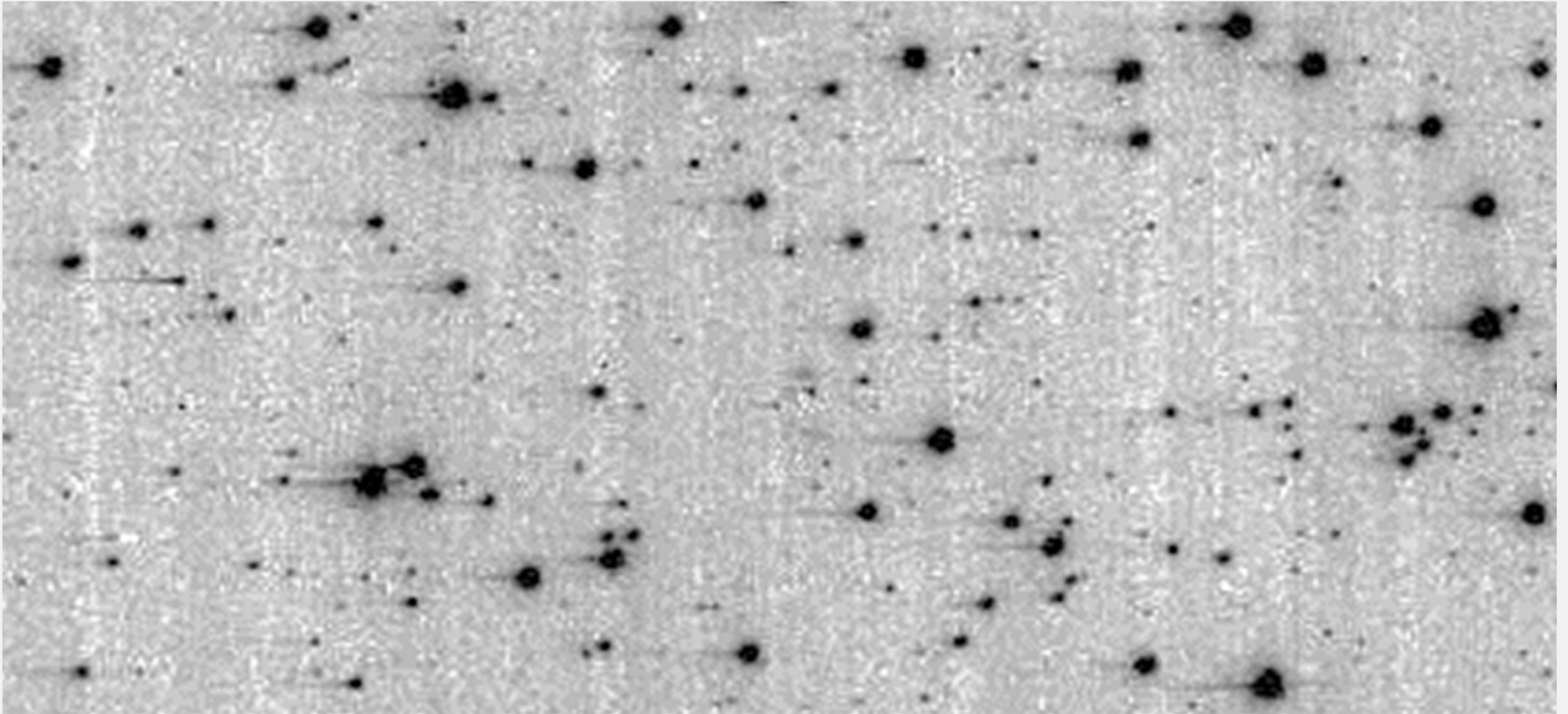
(W.L.Barnes, A.Dereux, T.W.Ebbesen: *Surface plasmon subwavelength optics*, Nature **424**, 824,2003)

Efficiency curves for diffraction gratings



Grating efficiency curves for a ruled diffraction grating in different linear polarizations
Blaze at 400 nm; 1200 grooves/mm (ThorLabs)

CCD limitations: Charge transfer [in]efficiency

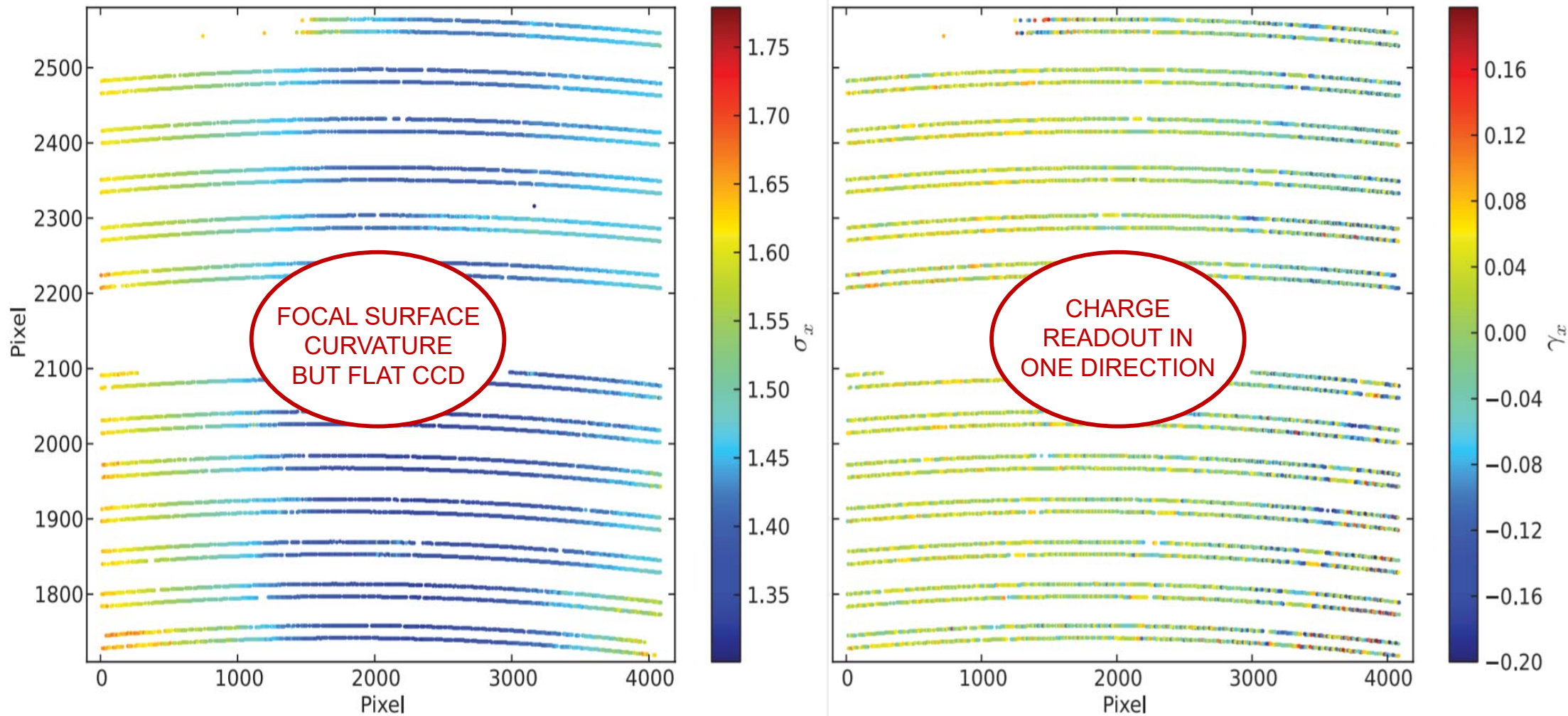


ACS, Advanced Camera for Surveys on Hubble Space Telescope

A section of an exposure of 47 Tucanae

Trails extending from the stars indicate effects of *Charge Transfer Efficiency* in the detector

Spectrometer instrumental profiles: HARPS



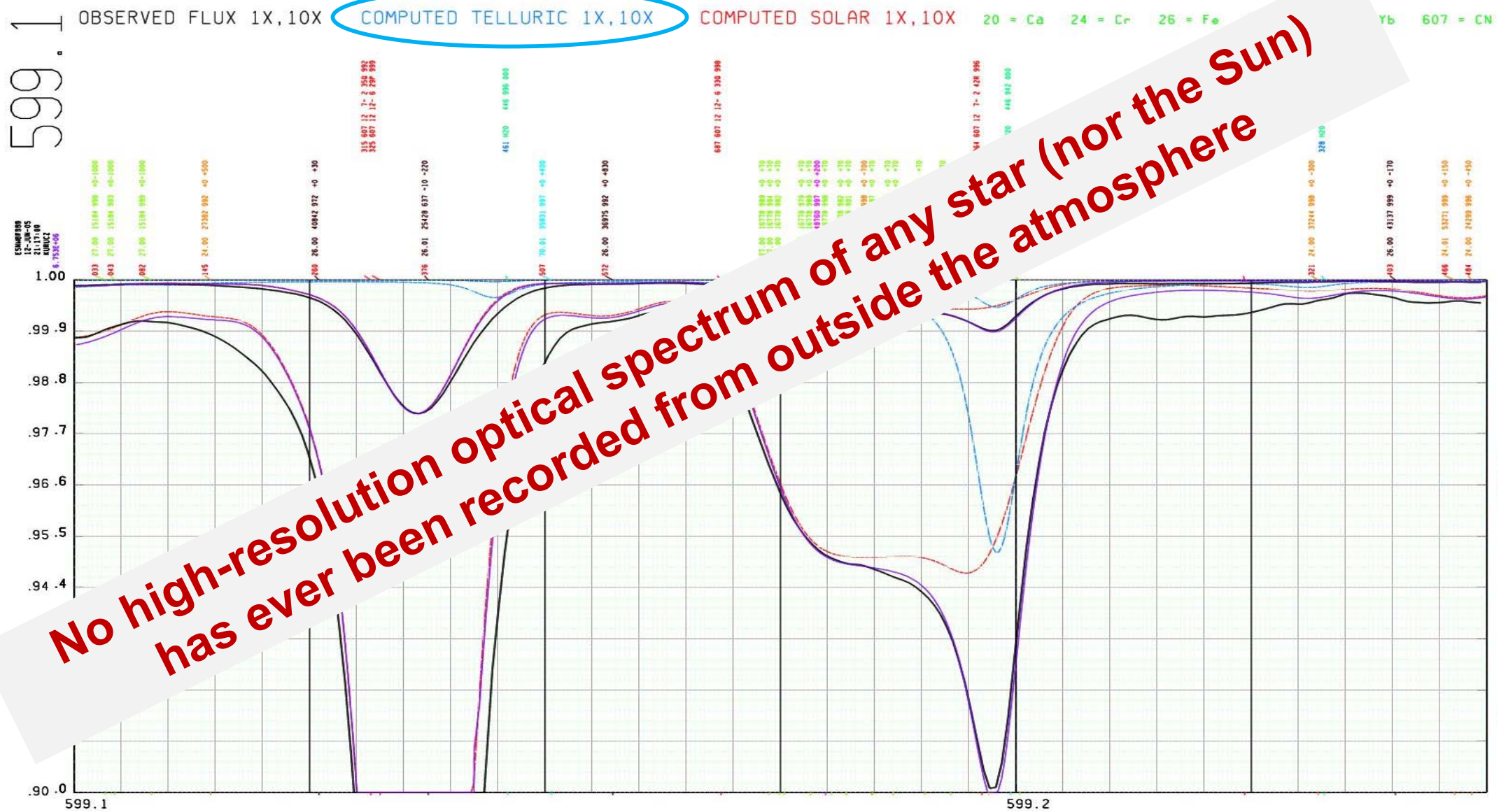
Laser comb spectrum of unresolved lines on the HARPS detector.

Left: Line width changes due to optical projection onto a flat CCD surface

Right: Line asymmetry (skewness) changes: presumably Charge Transfer Efficiency (CCD readout is off to the right). Asymmetry also depends also on the line intensity

Observing through the Earth's atmosphere

Precision limits from telluric absorption



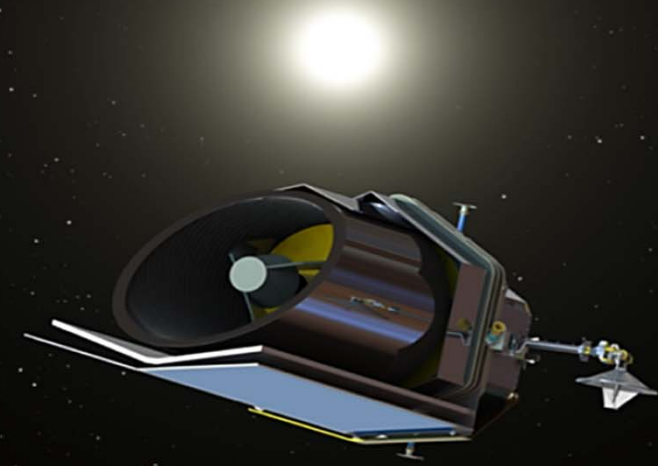
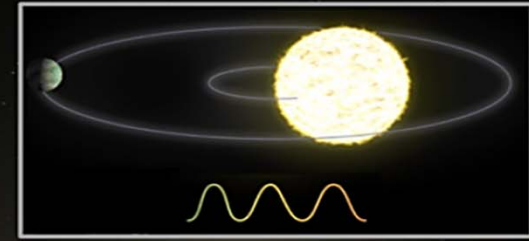
Example of a relatively empty region in the solar spectrum. Telluric, synthetic, and observed spectra at normal, and 10x scale.

Going to space to avoid telluric absorption ??

EarthFinder Probe Mission Concept Study

Characterizing nearby stellar
exoplanet systems with Earth-
mass analogs for future direct
imaging

March 2019



NASA Aeronautics and
Space Administration

PI: Peter Plavchan
George Mason University
Fairfax, Virginia

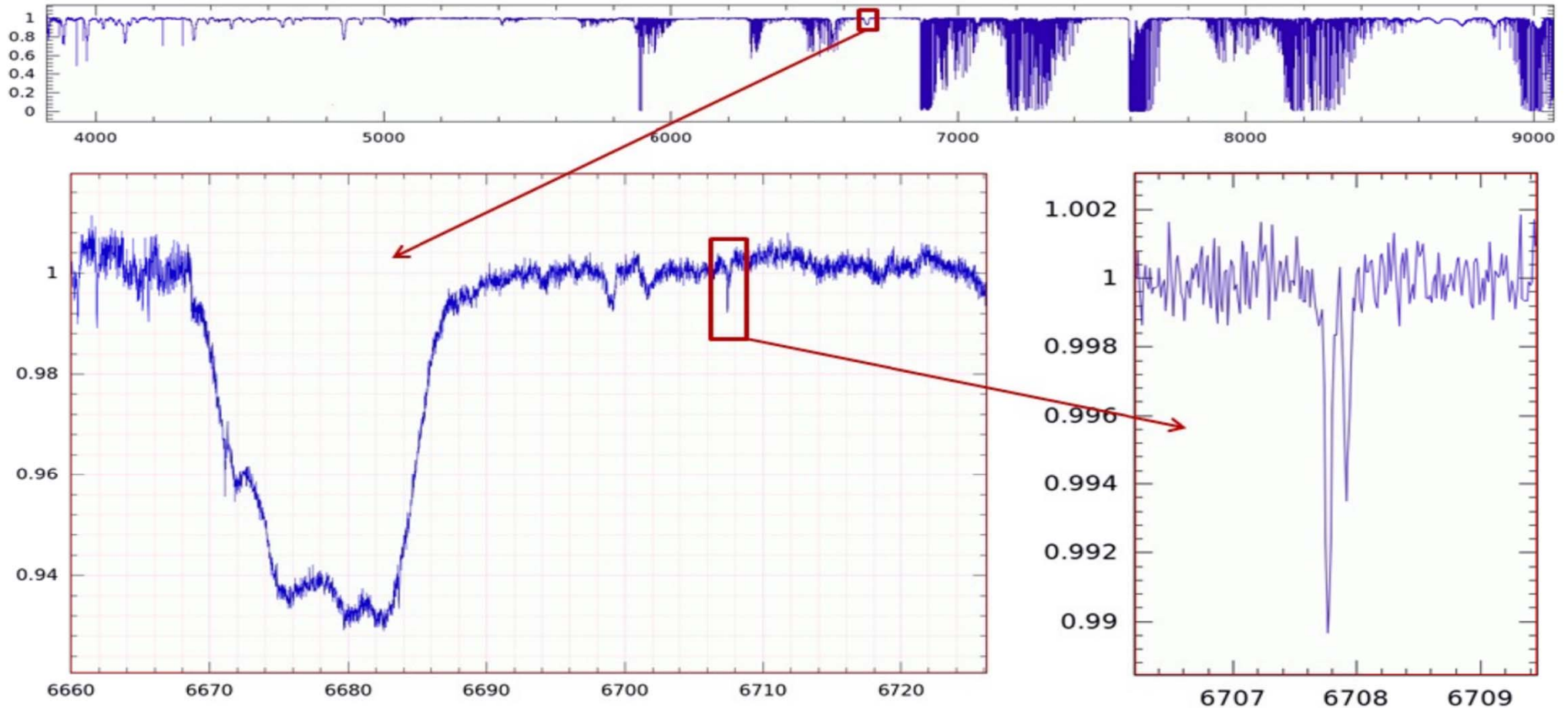
Co-I: Gautam Vasisht
Jet Propulsion Laboratory
California Institute of Technology
Pasadena, California

**Why do we
want fidelity?**

**What requires
 $S/N = 1,000$?**

PEPSI @ LBT

$\lambda/\Delta\lambda = 250,000, S/N = 1,800$



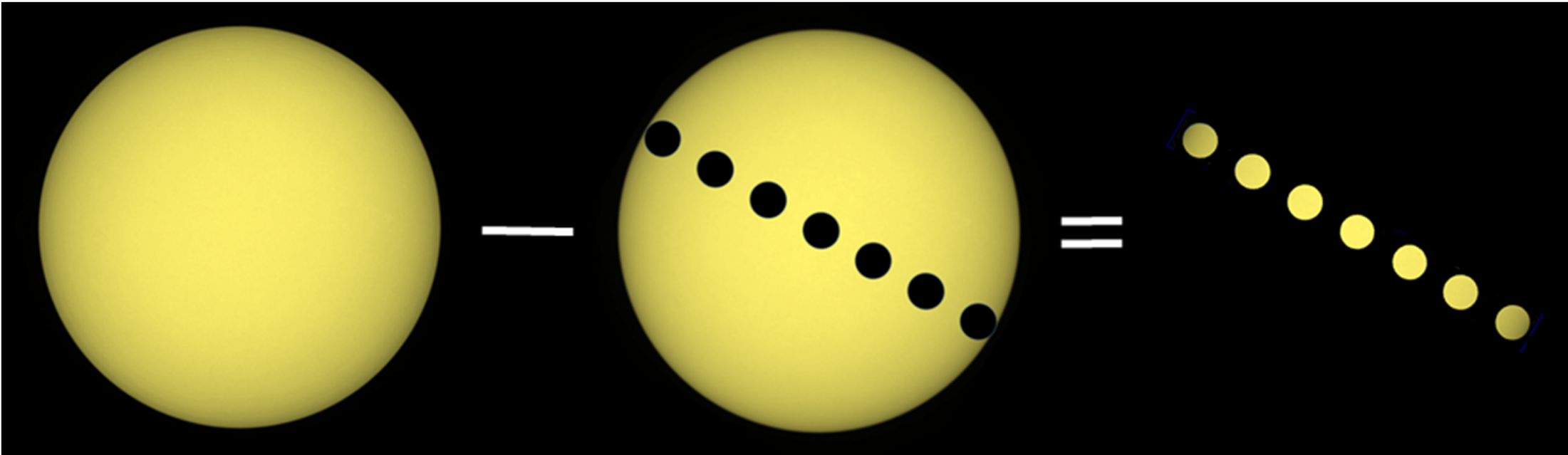
Interstellar lines in ζ Oph (O9 IV)

Left: Stellar He I 688 nm (deformed by non-radial pulsations)

Right: Resolved interstellar Li I doublet at 670.8 nm

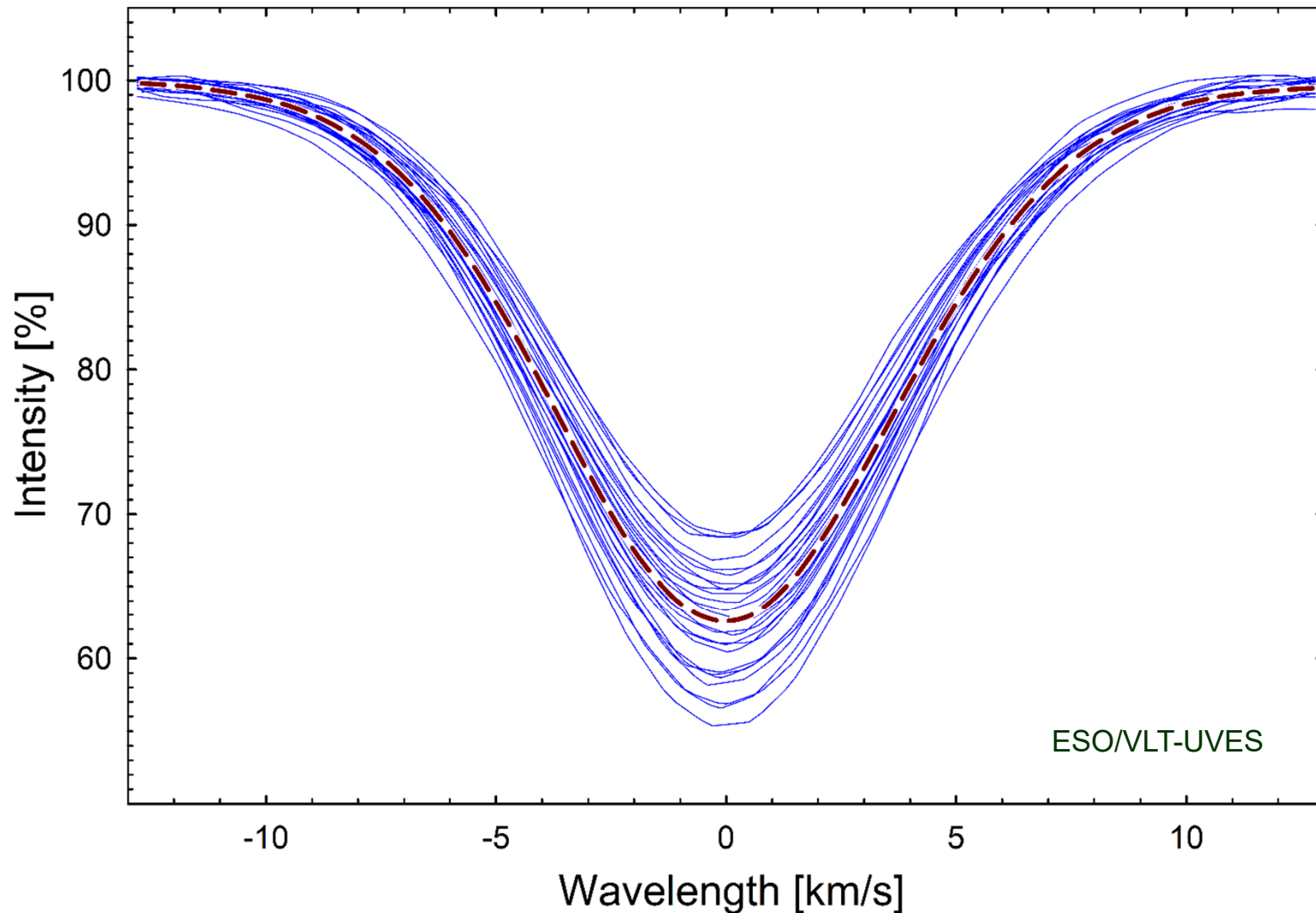
**What requires
 $S/N = 10,000$?**

Spatially resolved spectra across stellar surfaces



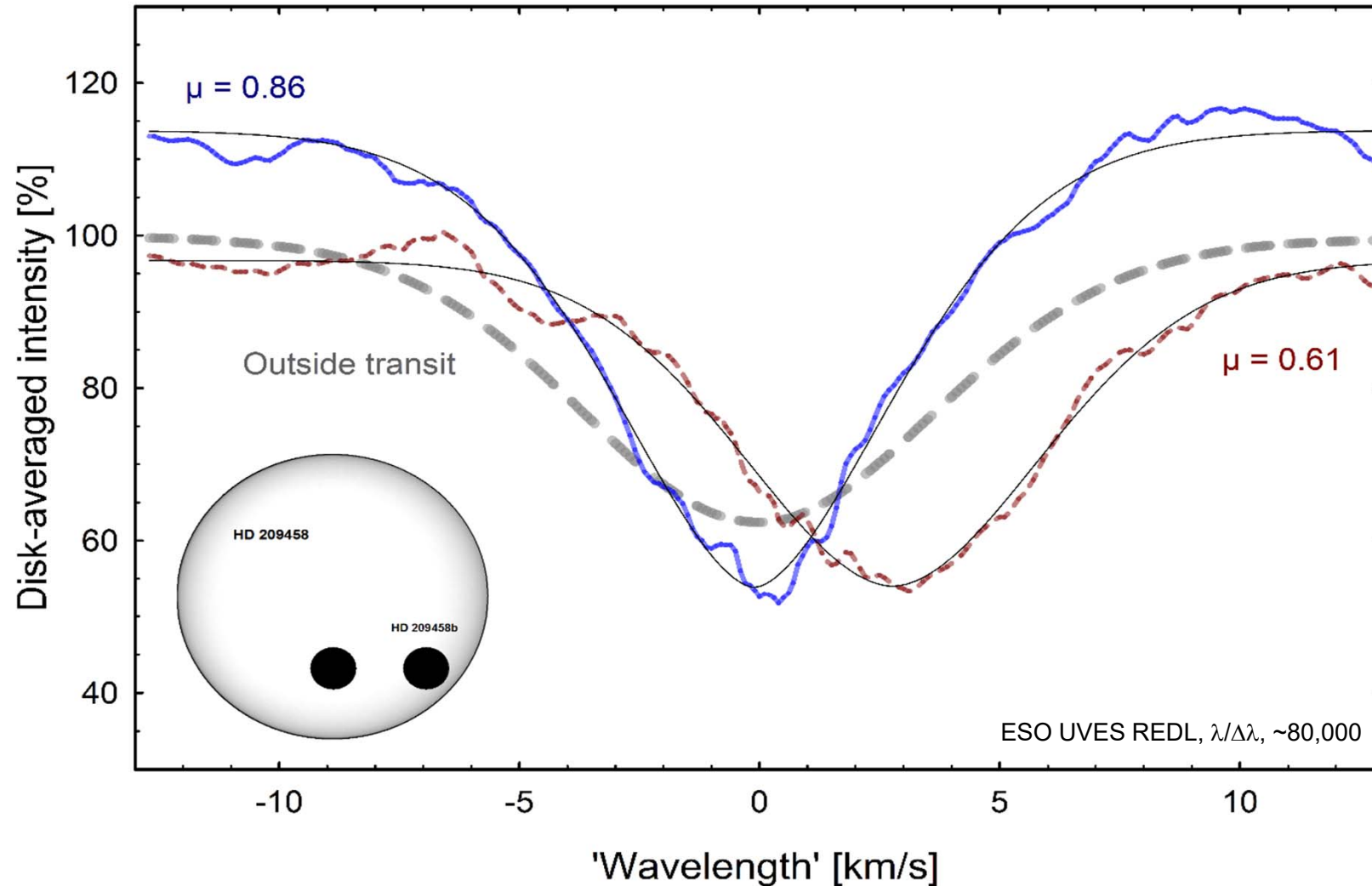
Differences during exoplanet transit reveal temporarily hidden stellar surface segments
Changing continuum flux measured by photometry, spectral changes by spectroscopy

Averaging many photospheric Fe I lines



Photospheric Fe I lines of similar strengths in HD 209458 carry redundant information
Averaging multiple exposures gives a representative profile with $\lambda/\Delta \lambda \sim 80,000$, S/N $\sim 7,000$

Retrieved line profiles across HD 209458 (G0 V)



Solid blue: near disk center, dashed brown: closer to limb.

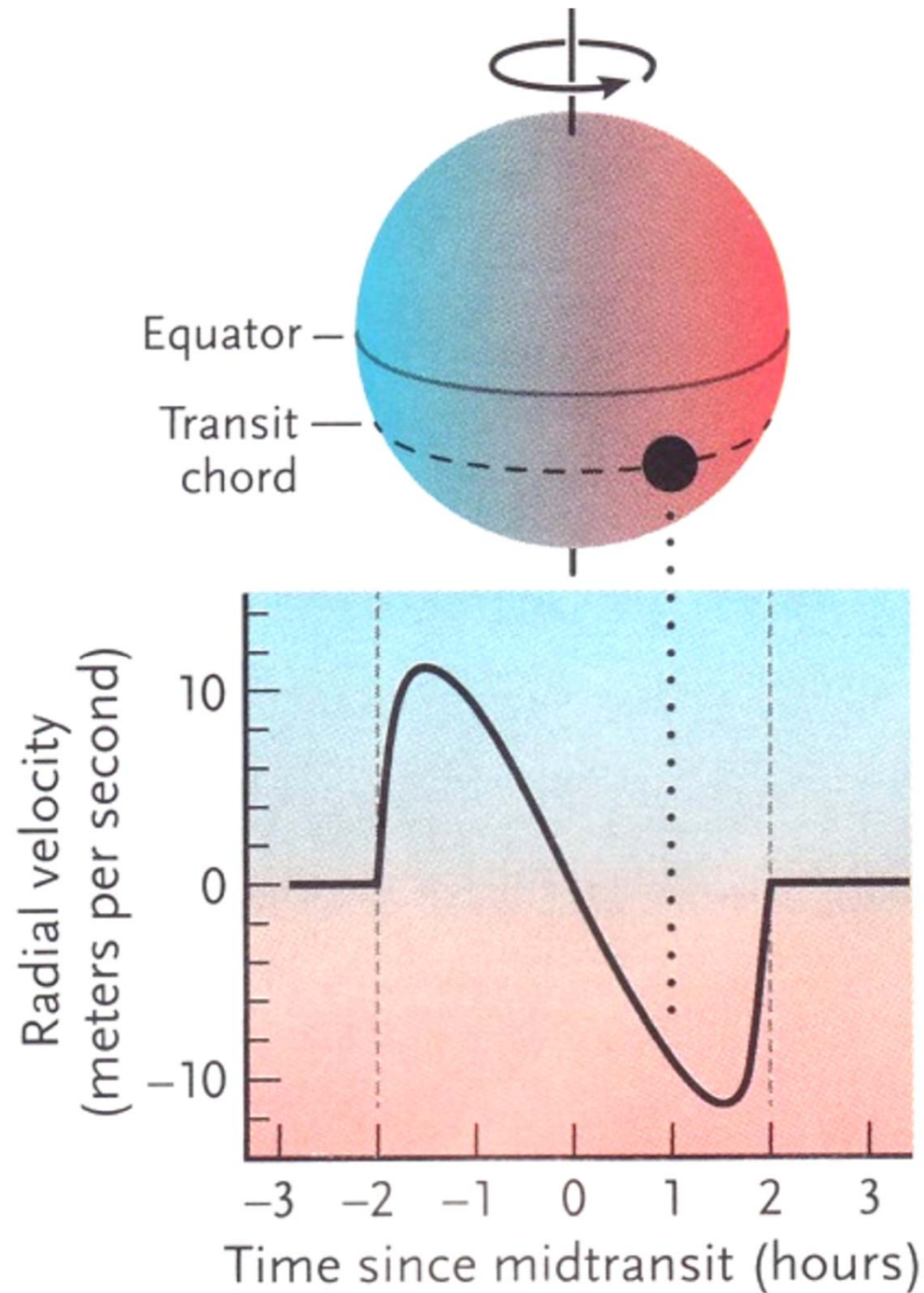
Spatially resolved lines are not rotationally broadened and are deeper than the disk average.

Wavelength shift during transit illustrates stellar rotation and prograde orbital motion of the exoplanet.

Planet size and positions on the stellar disk are to scale.

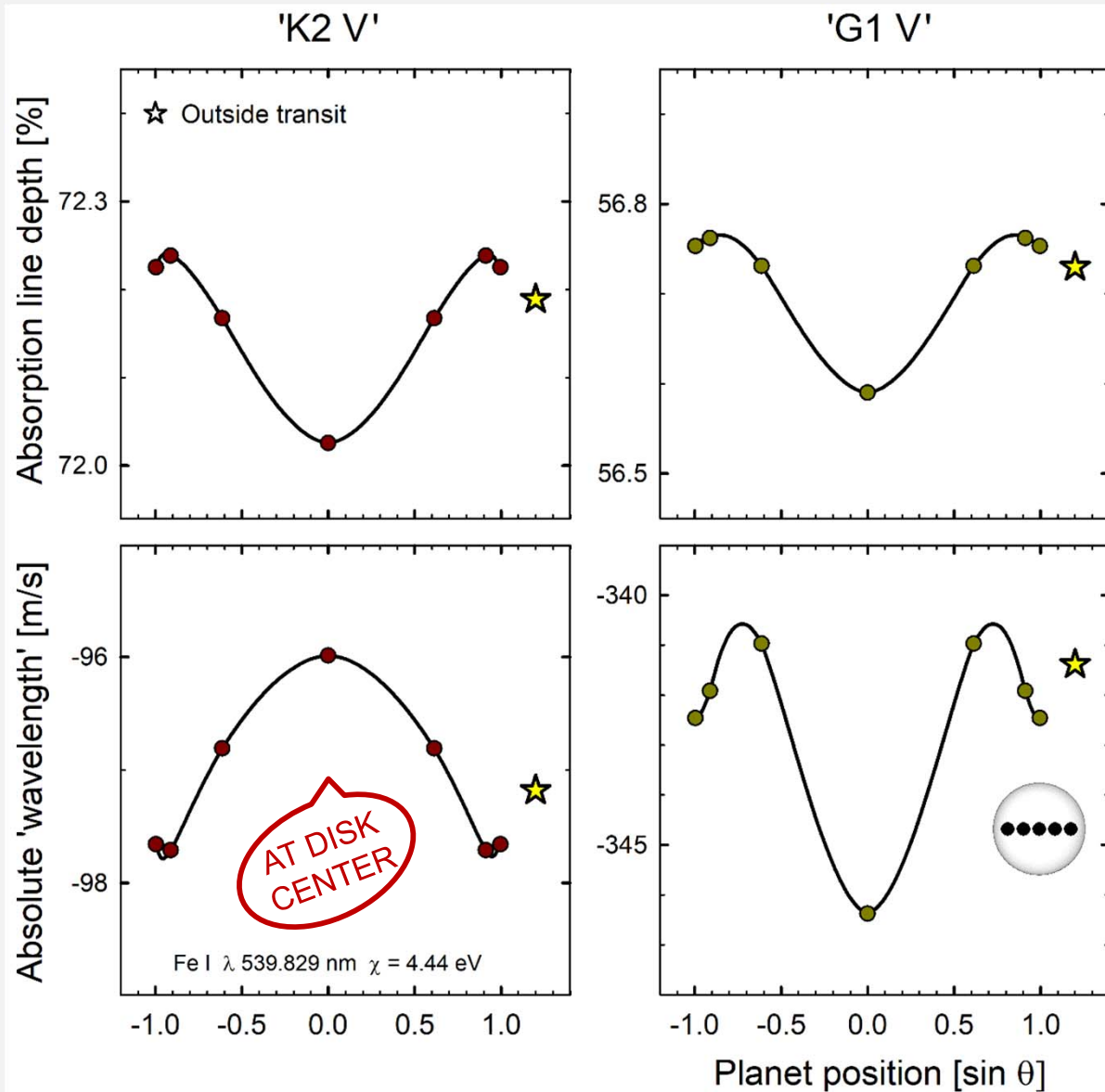
**Exoplanet transits:
Stellar center-to-limb
line profile changes**

Classical Rossiter-McLaughlin effect



Analogies to the Rossiter-McLaughlin effect

Exoplanet transit signatures



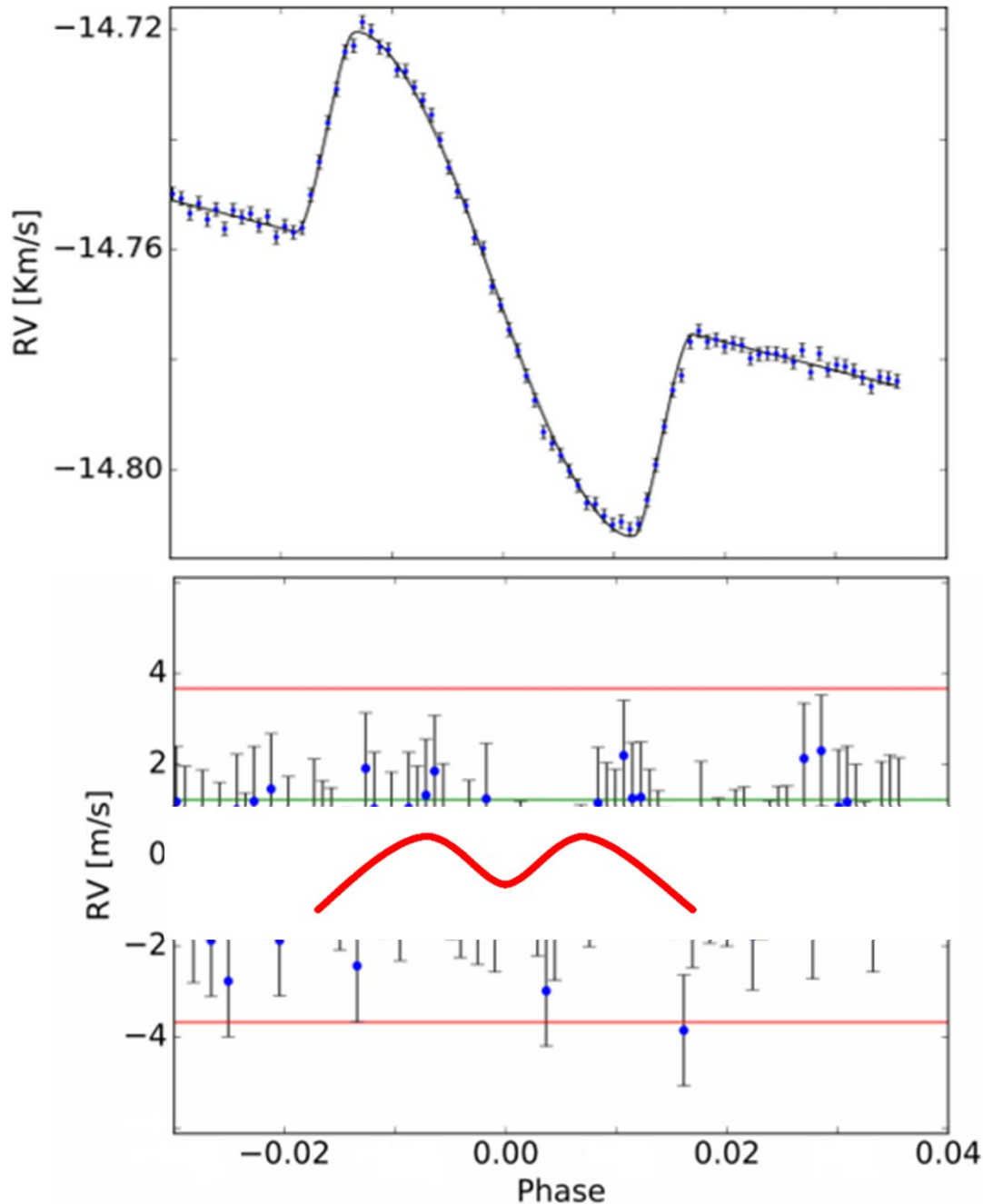
Changes during exoplanet transit, caused by center-to-limb line profile changes, **in absence of stellar rotation**

Modeled transit across a stellar diameter of an exoplanet covering 1.5% of the stellar disk

Star symbols denote full-disk values outside transit.

Wavelength shifts are absolute but gravitational redshifts are neglected

Observed effects across HD 209458 at $\lambda/\Delta\lambda = 140,000$



ESPRESSO transit observations vs. orbital phase

Top: Rossiter–McLaughlin curves and best-fit models

Bottom: Residuals from best fit for the night with best S/N

N.C.Santos et al.:

Broadband transmission spectroscopy of HD 209458b with ESPRESSO: evidence for Na, TiO, or both?

Astron. Astrophys. **644**, A51 (2020)

Overlay: Predicted radial-velocity signature, caused by intrinsic changes of the line asymmetry and convective wavelength shift when going from stellar disk center toward the limb.

For medium-strong Fe I lines, a maximum redshift of some m/s, about halfway between disk center and the limb is expected, seemingly consistent with the observed R-M deviations.

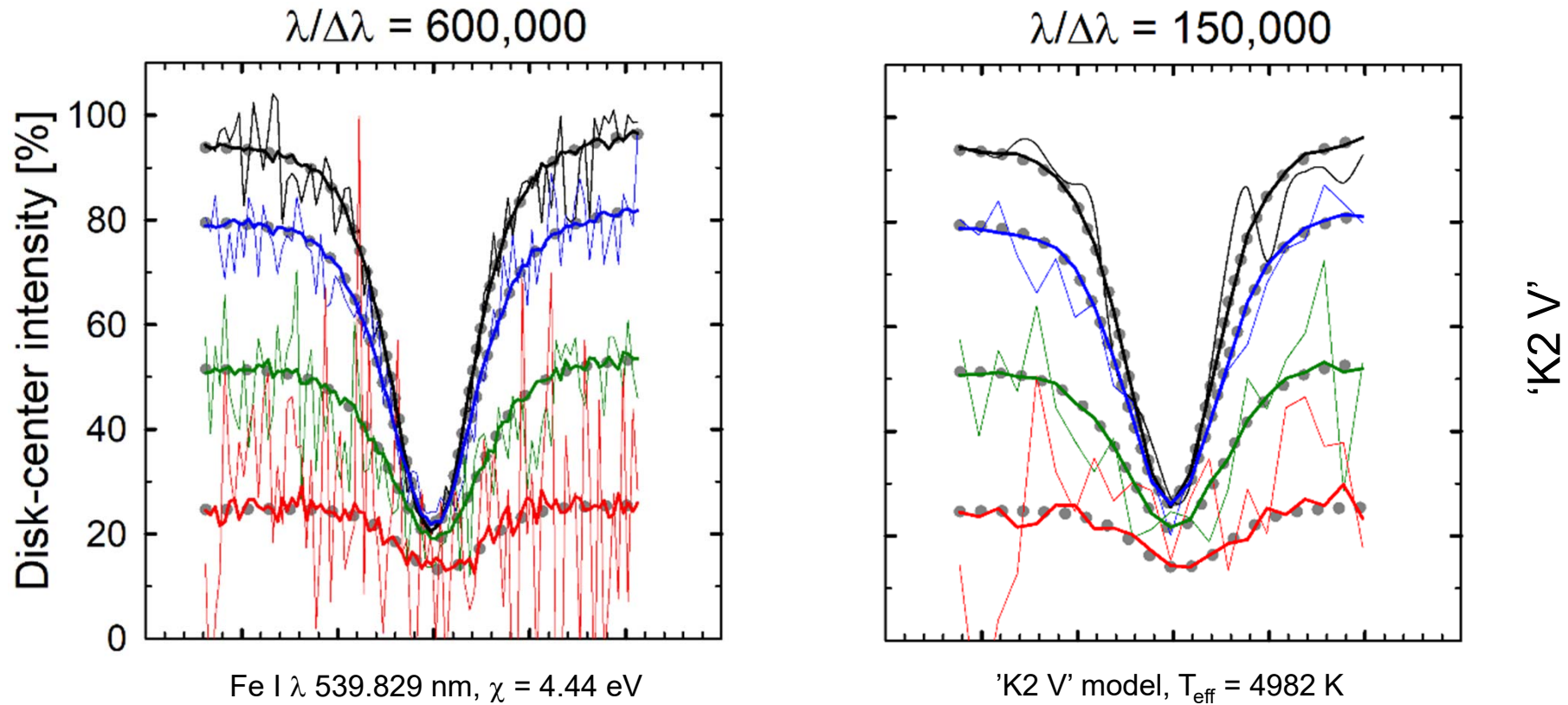
Overlay modeling:

D.Dravins, H.-G.Ludwig, B.Freytag: *Spatially resolved spectroscopy across stellar surfaces. V. Observational prospects: Toward Earth-like exoplanet detection*, *Astron.Astrophys.* **649**, A17 (2021)

D.Dravins, H.-G.Ludwig, in preparation (2023)

**What could be done
with $S/N = 100,000$?**

Retrieving spatially resolved spectra



Simulated reconstructions from transit of an exoplanet covering 1.5% of a stellar disk

Spectral resolutions: $\lambda/\Delta\lambda = 600,000$ & $150,000$

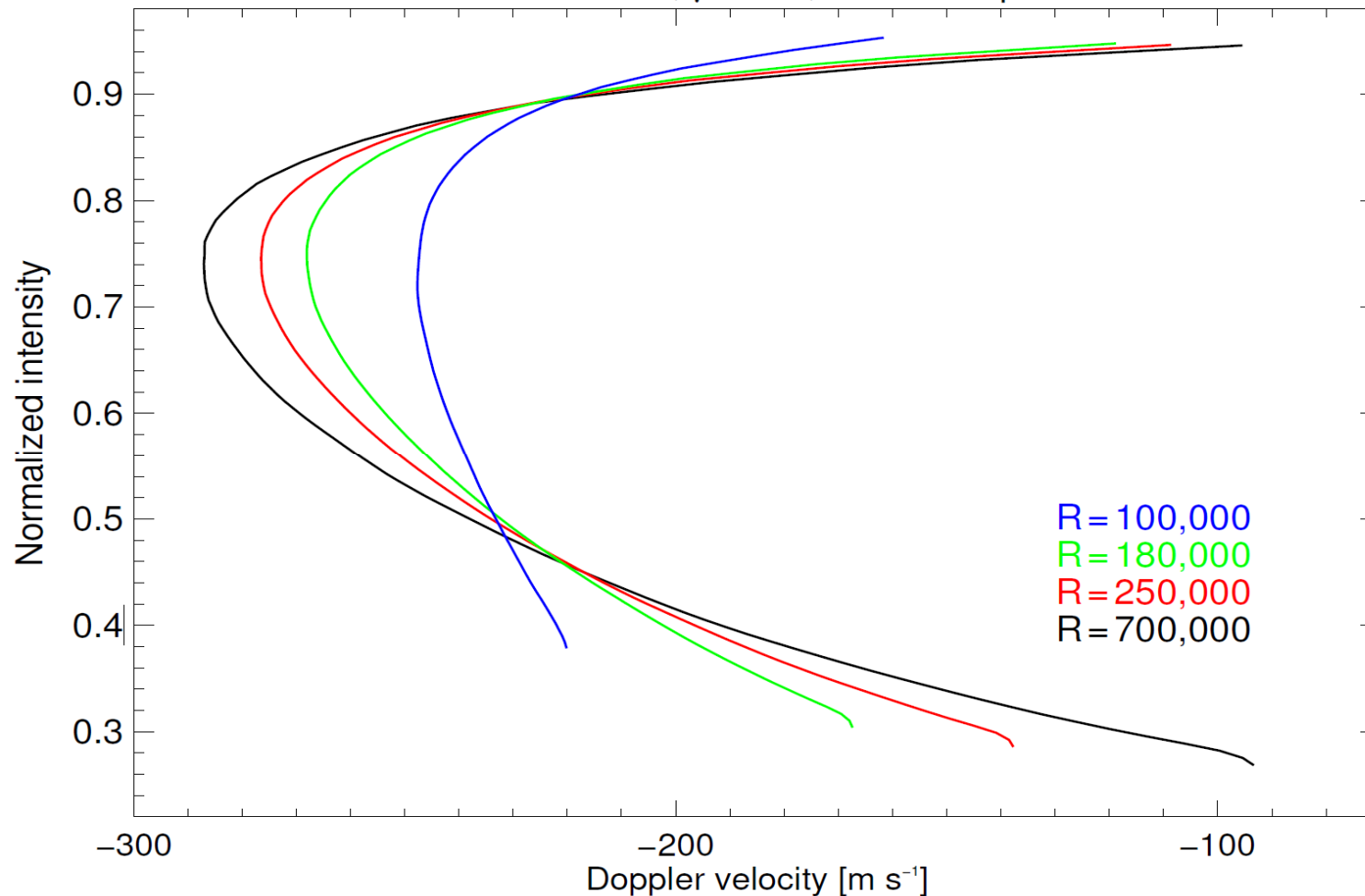
Photometric S/N = 10,000 (thin lines), S/N = 100,000 (bold). Noise-free original: gray dots.

From top down: $\mu = 1, 0.79, 0.41, 0.09$

What requires
 $\lambda/\Delta\lambda = 1,000,000$?

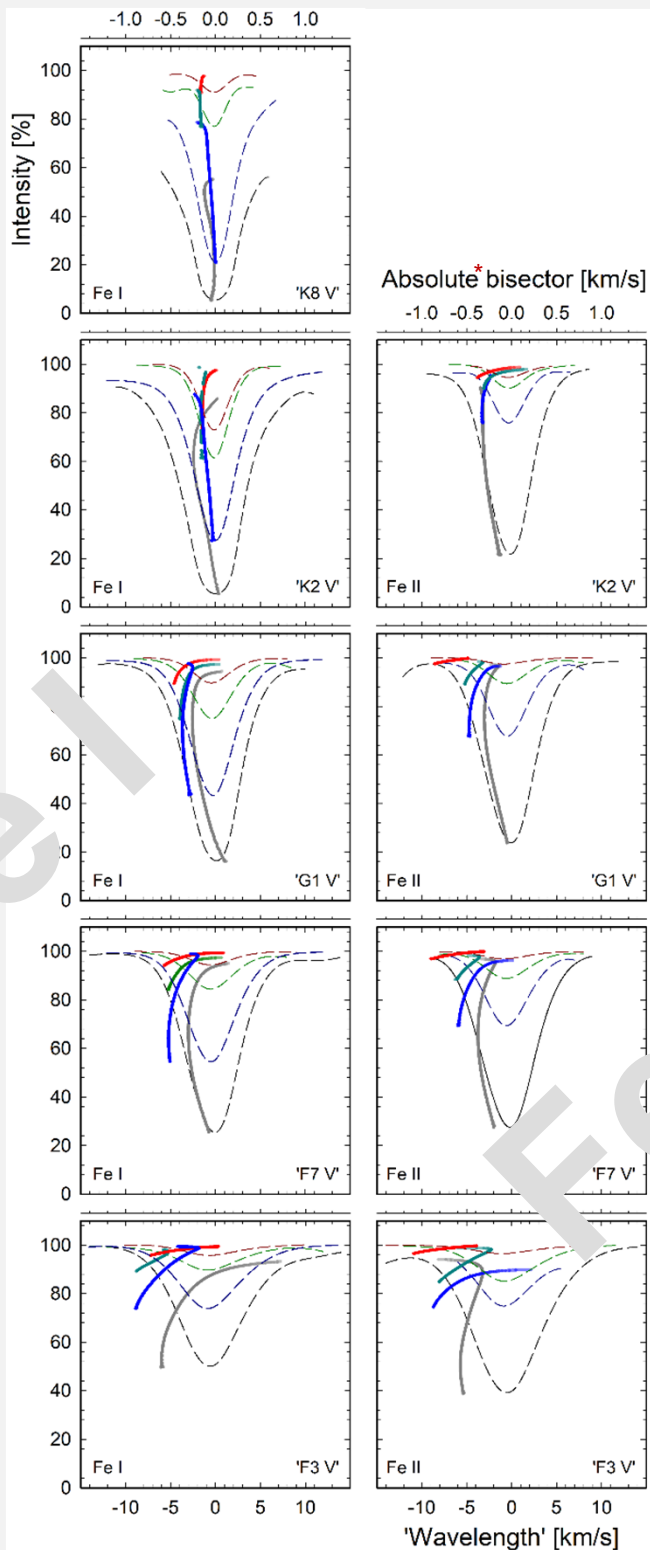
Need for hyper-high spectral resolution

Solar spectral lines observed at different $\lambda/\Delta\lambda$



Bisector changes with spectral resolution

Fe I 525.02084 nm for $\lambda/\Delta\lambda = 700,000$ (black) to 100,000 (blue)



Bisectors for different spectral types

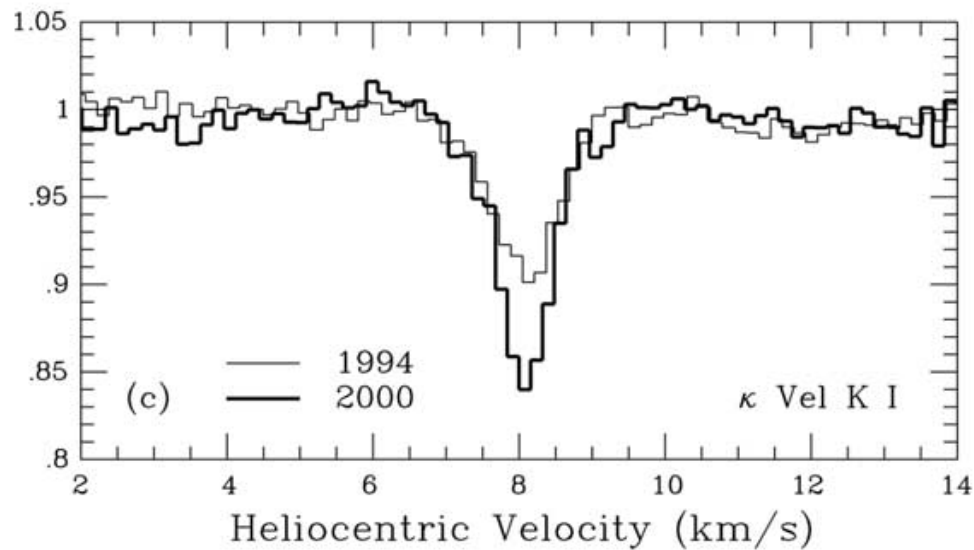
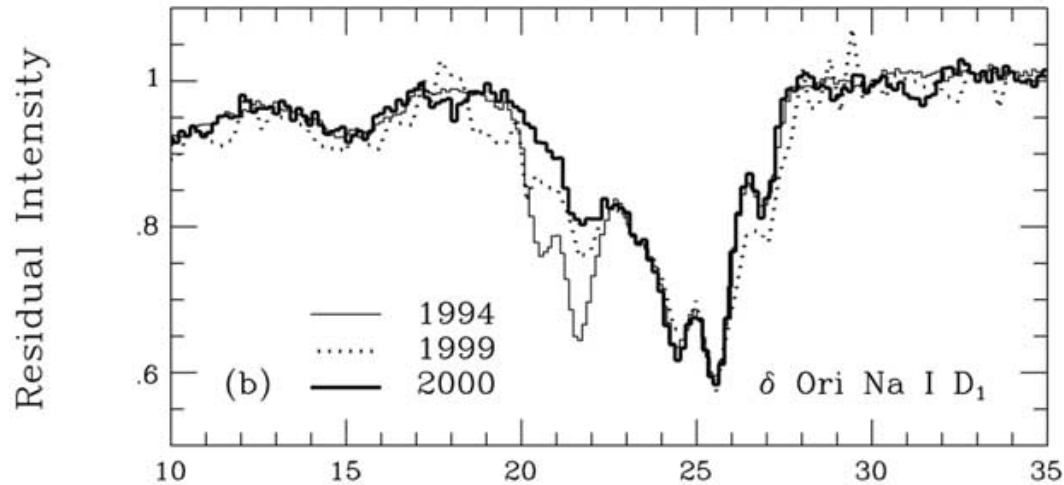
Synthetic line
profiles and
bisectors in
integrated
starlight

$$\lambda/\Delta\lambda \approx 1,100,000$$

D.Dravins, H.-G.Ludwig, B.Freytag:
*Spatially resolved spectroscopy across stellar surfaces. IV.
F, G, & K-stars: Synthetic 3-D spectra at hyper-high resolution*
Astron.Astrophys. **649**, A16 (2021)

Interstellar line variability

Ultra High-Resolution Facility @ AAT, $\lambda/\Delta\lambda = 940,000$

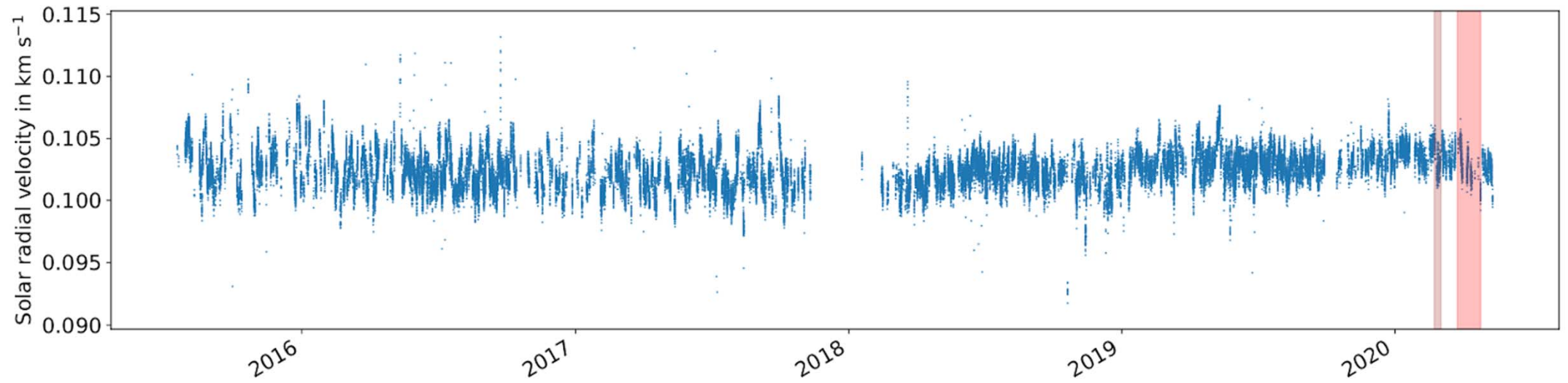


*Variable interstellar lines,
also resolving the Na I D₁
hyperfine structure
(separation 1.08 km/s)*

*Variation over years imply
scales on 10-100 AU*

Temporal microvariability

Radial velocity jittering of the Sun



Solar apparent radial velocity at 5-minute cadence, corrected for barycentric motion and differential extinction

Colored bars indicate the 2020 Calima sandstorm and the COVID-19 lock-down. (Credit: A.Collier Cameron)

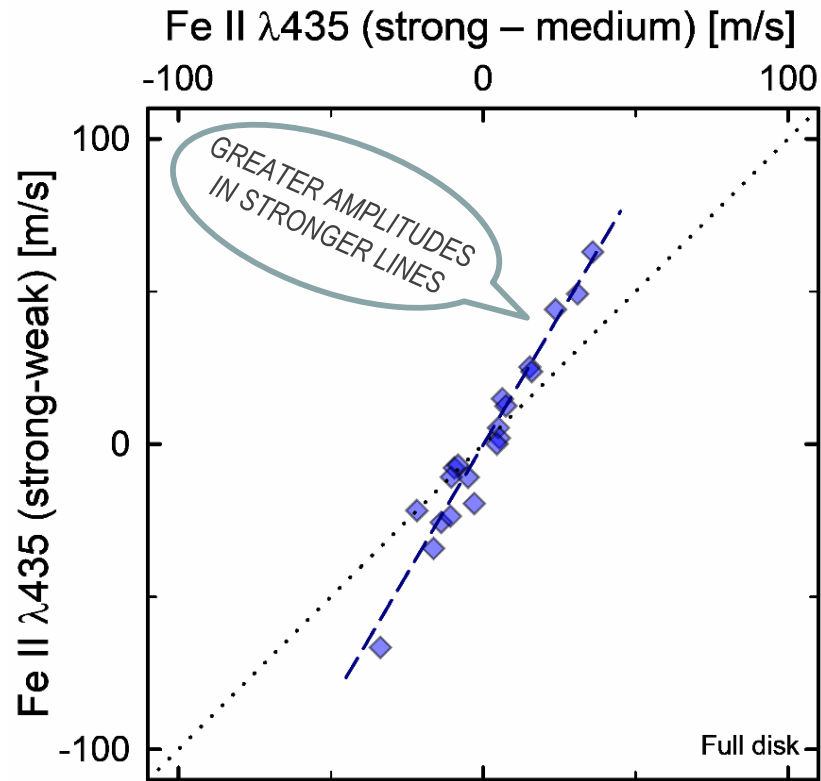


Telescopio Nazionale Galileo (TNG)
Roque de los Muchachos, La Palma

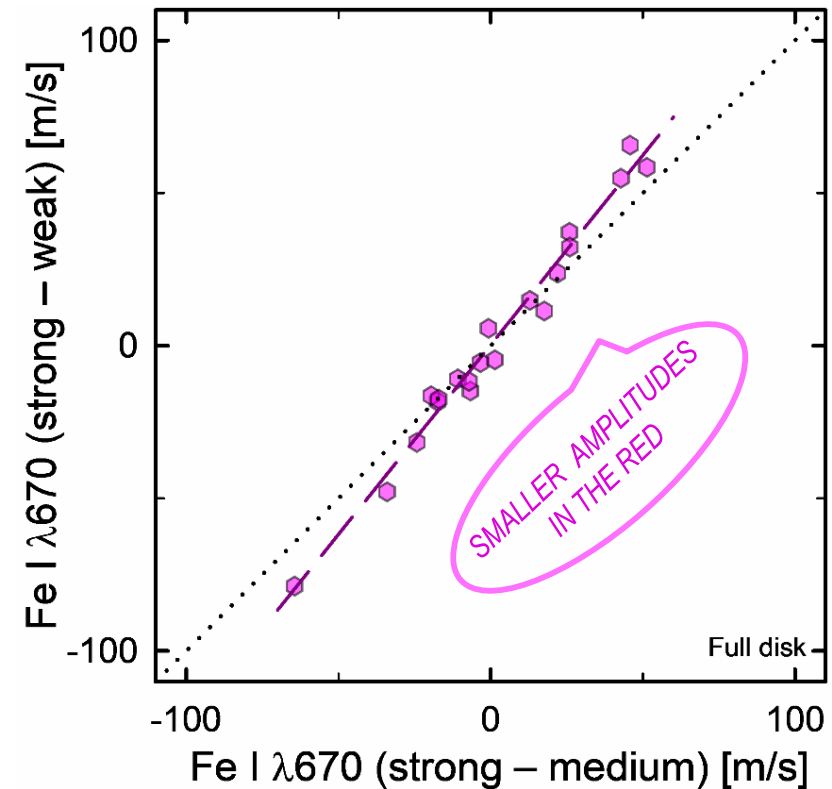
Data release: X. Dumusque et al.: *Three Years of HARPS-N High-Resolution Spectroscopy and Precise Radial Velocity Data for the Sun*, *Astron.Astrophys.* **648**, A103 (2021)

Solar telescope feeding the HARPS-N spectrometer (credit: D.Phillips)

Velocity jittering due to solar granulation



ΔV – MORE DIFFERENT LINES



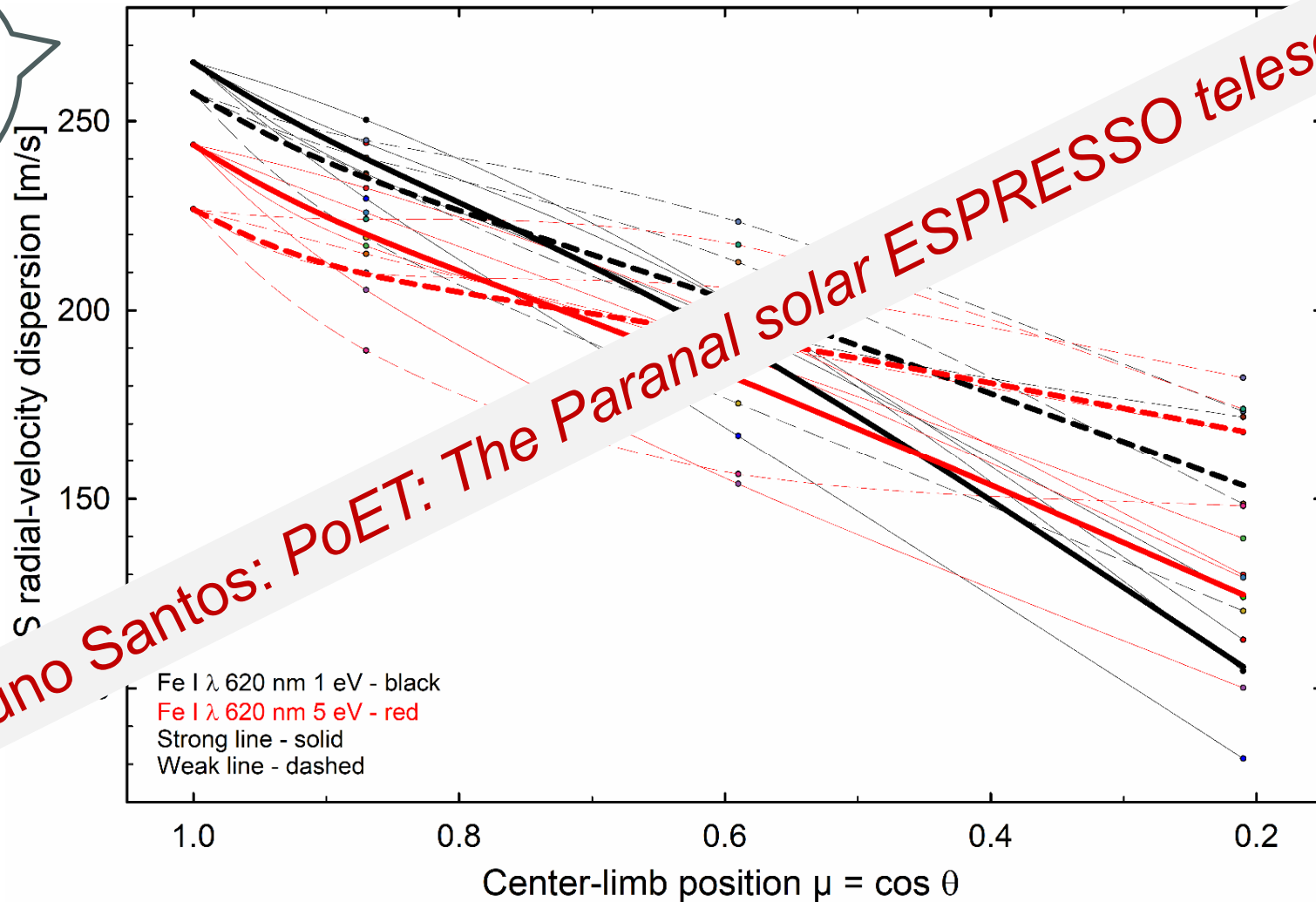
ΔV – SLIGHTLY DIFFERENT LINES

Radial-velocity excursions are greater for stronger and for ionized lines, decreasing at longer wavelengths

Numbers [m/s] refer to a small simulation area; for full-disk Sun, divide by ~ 150 - 200 : amplitude ~ 2 m/s

'Radial velocity' jittering across solar disk

DISK CENTER



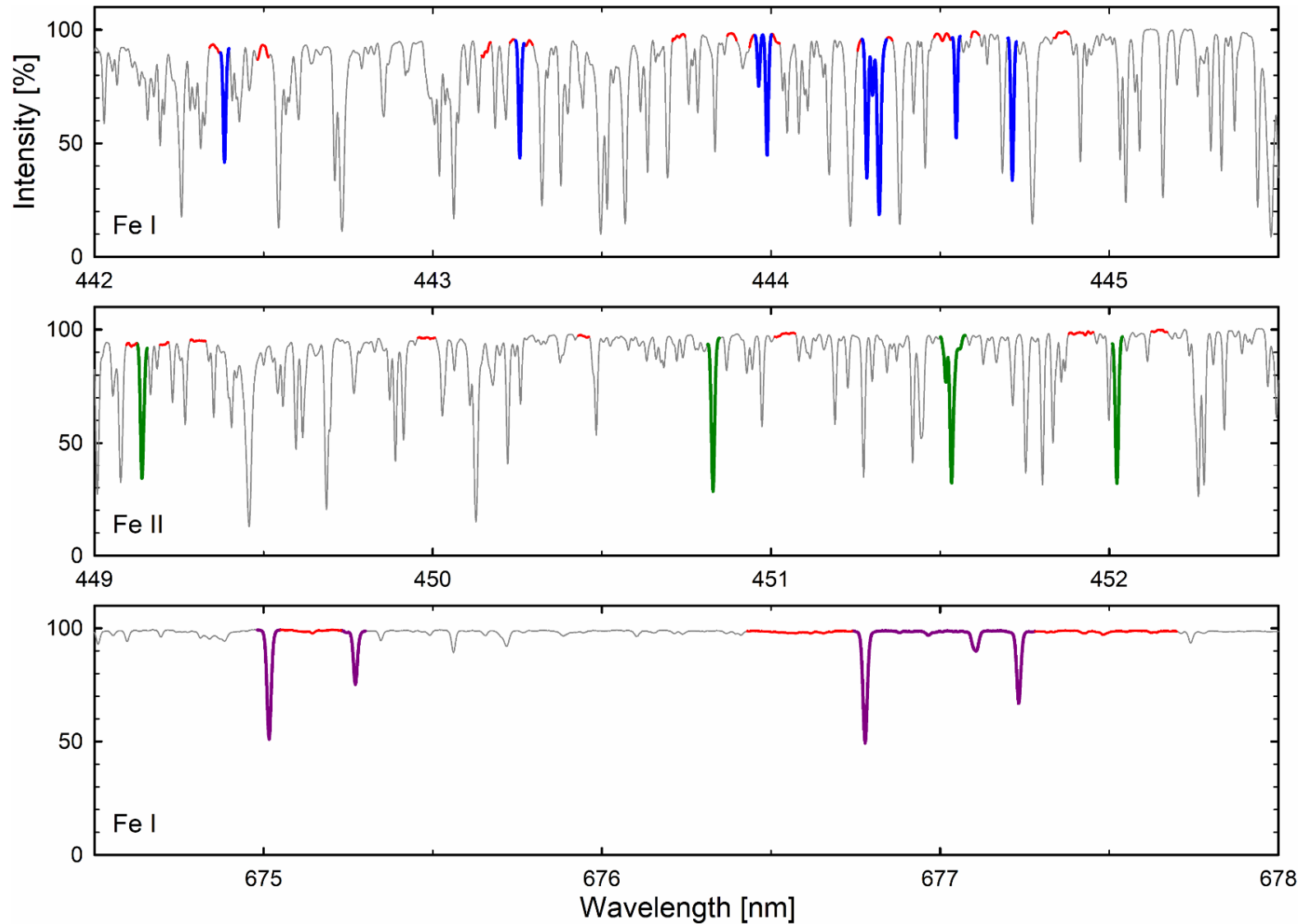
Talk by Nuno Santos: PoET: The Paranal solar ESPRESSO telescope

CLOSE TO LIMB

Theoretically predicted jittering of Fe I λ 620 nm lines due to granulation

**Extreme precision radial-velocity
spectrometers enable extreme
precision stellar spectroscopy**

Fe I and Fe II lines @ HARPS-North



**Selected Fe lines in
different spectral
regions**

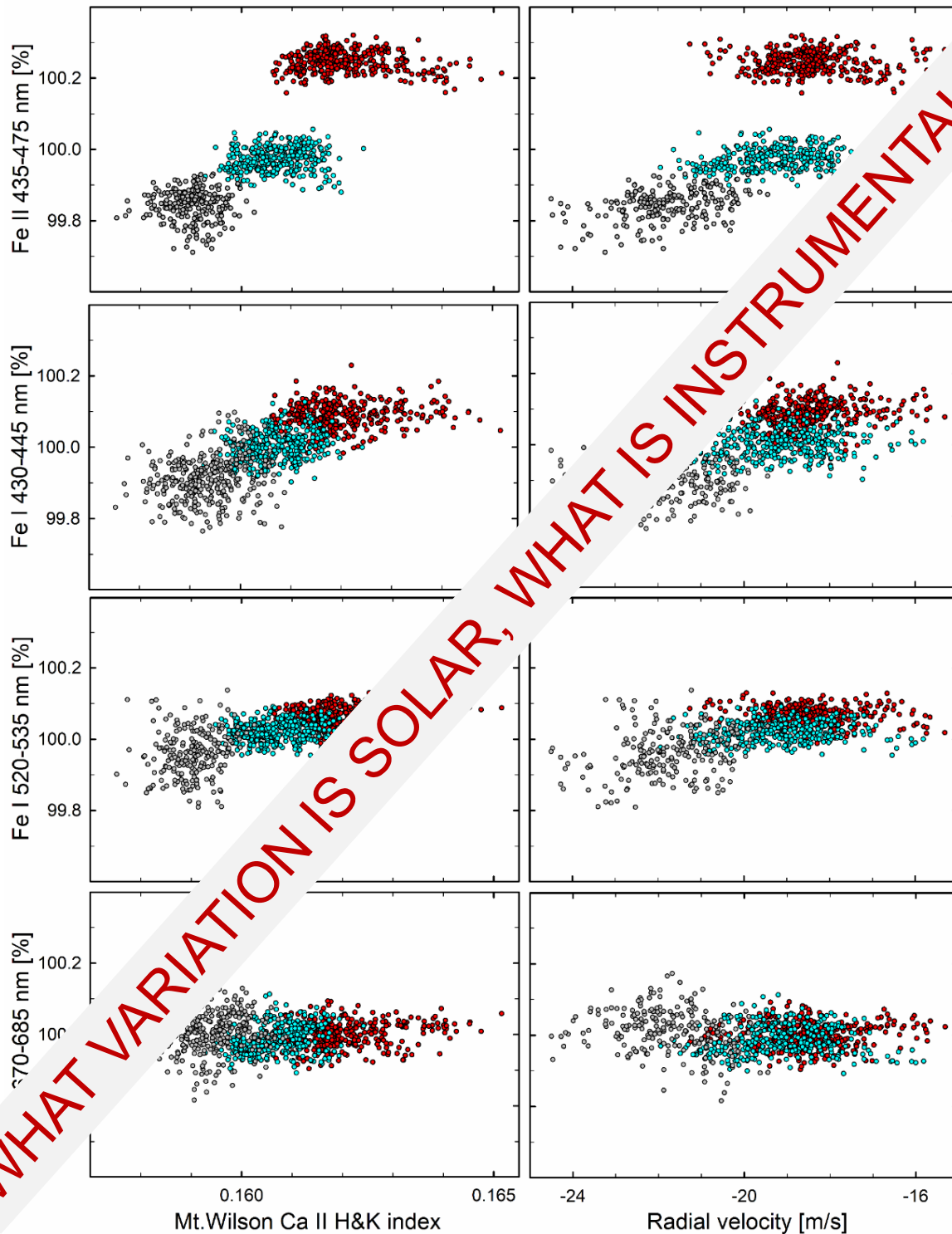
Red: Reference “continua”

Thin: 100-exposure average

D.Dravins, H.-G.Ludwig, *to be submitted* (2023)

Data from X.Dumusque et al.: *Three Years of HARPS-N High-Resolution Spectroscopy and Precise Radial Velocity Data for the Sun*
Astron.Astrophys. **648**, A103 (2021)

Fe line fluxes @ HARPS-North



2016
2017
2018

Fe I and Fe II fluxes
vs. Ca II H & K (left);
vs. radial velocity (right)

D.Dravins, H.-G.Ludwig, *to be submitted* (2023)

Data from X.Dumusque et al.: *Three Years of HARPS-N High-Resolution Spectroscopy and Precise Radial Velocity Data for the Sun* *Astron.Astrophys.* **648**, A103 (2021)

**What requires cm/s
radial-velocities?**

Gravitational redshift within the solar atmosphere



$h = 1000$ km, 635.396 m/s



$h = 100$ km, 636.219 m/s



$h = 0$, 636.310 m/s

**Line asymmetries
and convective
wavelength shifts**

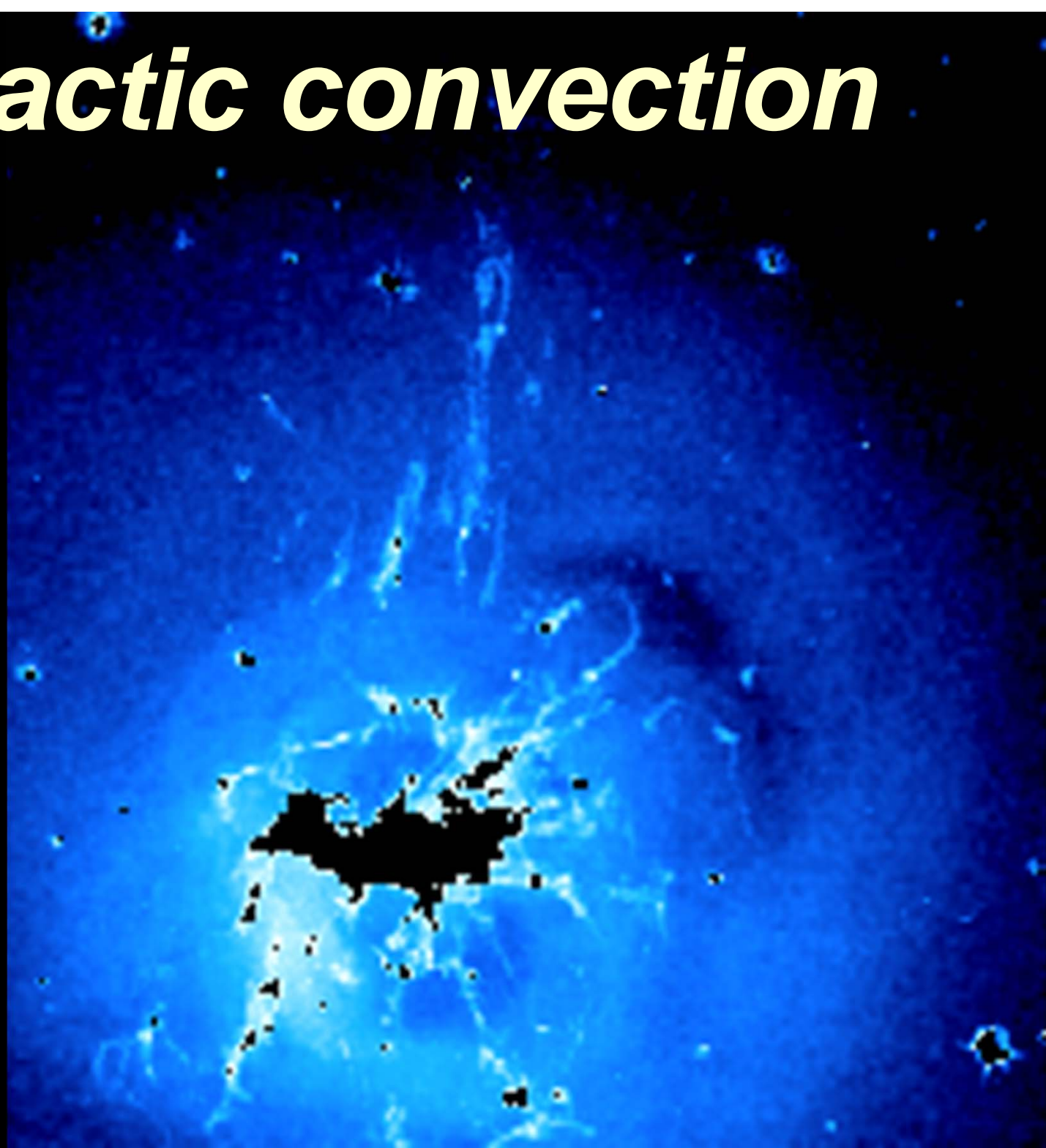
Intergalactic convection

Perseus cluster core in X-rays
overlaid with H α image

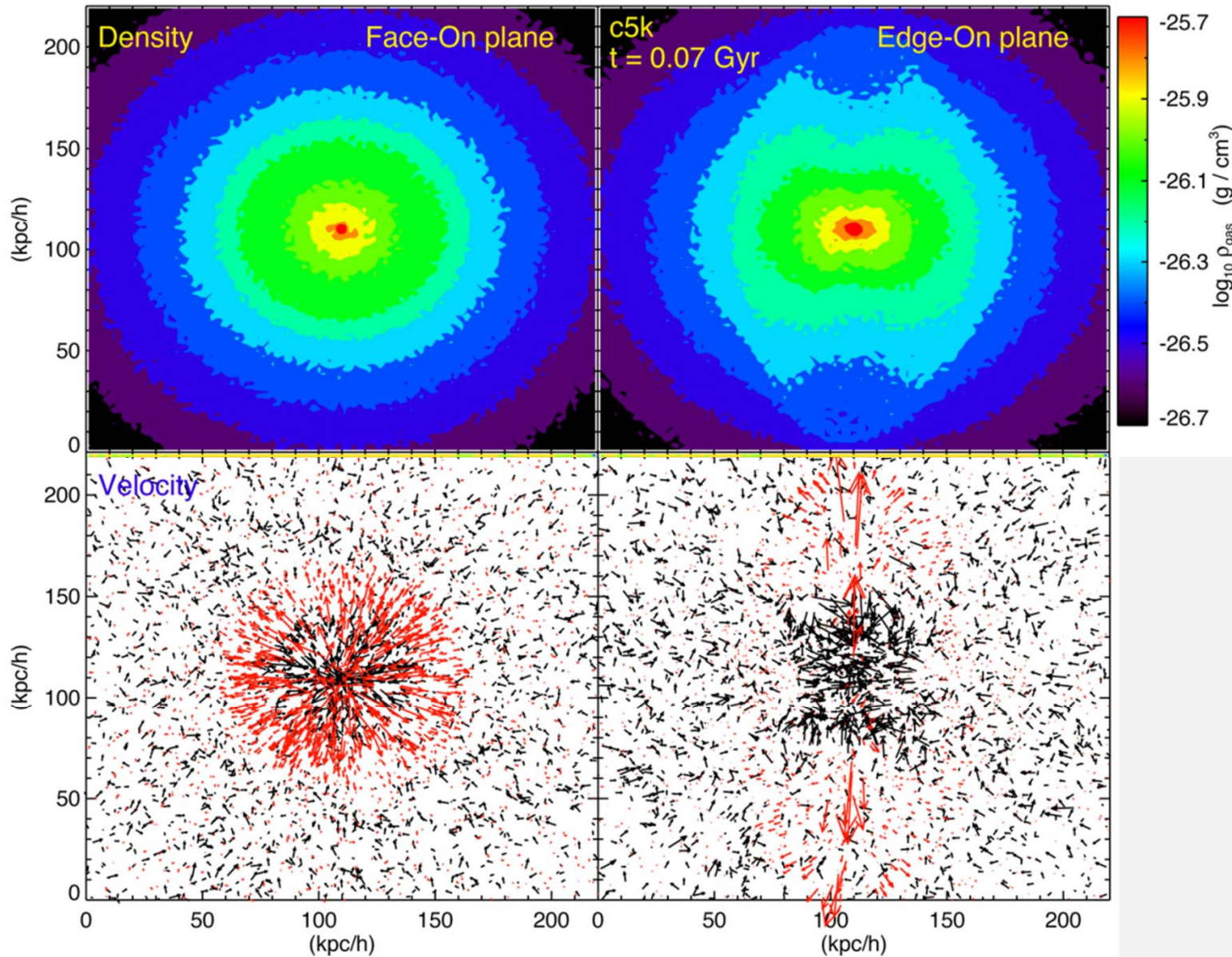
Arc-shaped H α filaments suggest
vortex-like flows

Image is 96 kpc on the side

Reynolds et al.: *Buoyant radio-lobes
in a viscous intracluster medium,*
MNRAS **357**, 242 (2005)



Intergalactic convection



AGN feedback, modeled with smoothed-particle hydrodynamics

A black hole at the cluster center ejects energetic hot gas

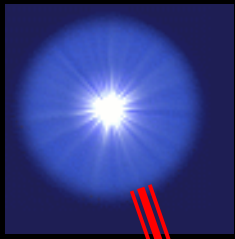
Fast wind shocks slower-moving gas, bubble-like outflows propagate out to a distance of a few 100 kpc.

Inclusion of cold gas accretion produces a duty cycle of the AGN with a periodicity of ~ 100 Myr.

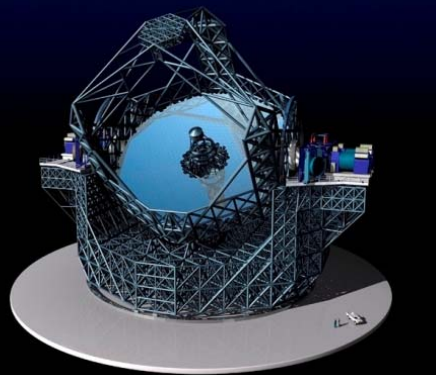
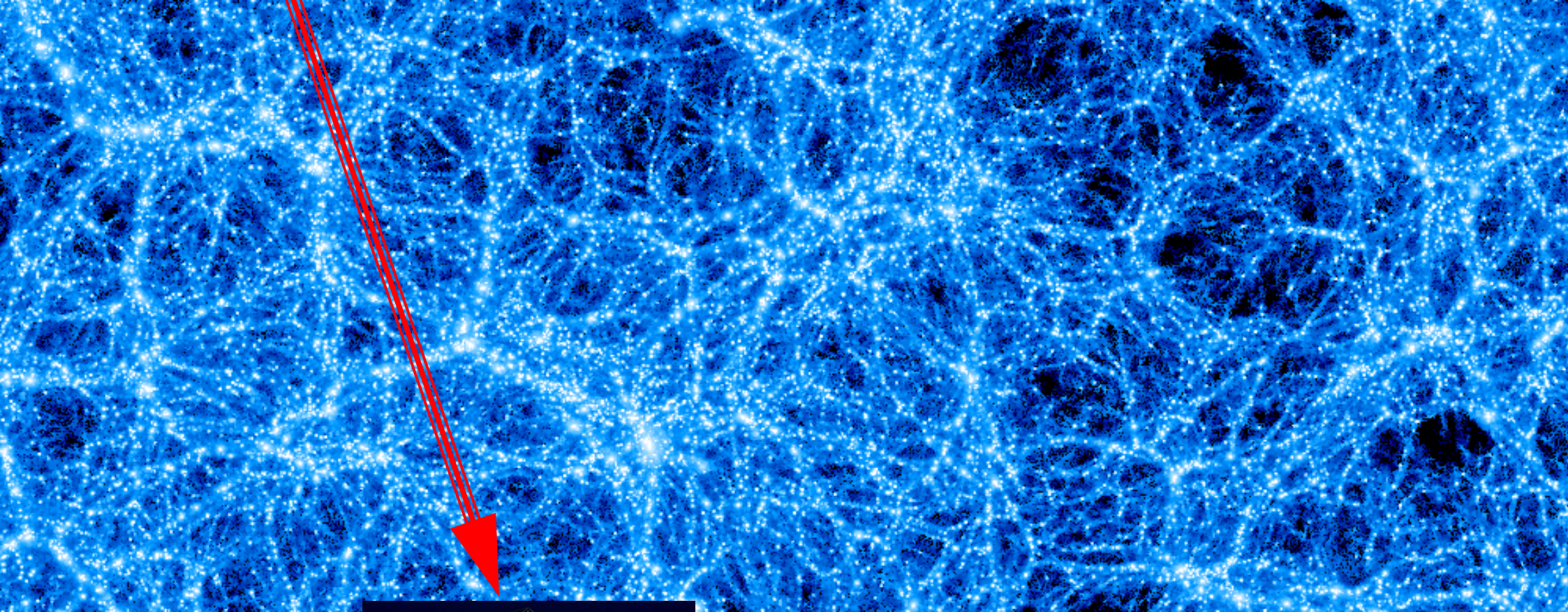
Top: 2D projection of gas kinematics face-on and edge-on for a $(200 \text{ kpc/h})^3$ volume around the cluster center

Bottom: Velocity vectors with outflow ($v_r > 0$) marked red, and inflow black

QSO



Observing the intergalactic medium



Cosmological 3-D hydrodynamic simulation. Density map; each bright point is a group of galaxies evolved within CDM cosmology. Image width = 400 Mpc.
(James Wadsley)

**Toward the
post-CCD era
in spectroscopy**

CCD: Current standard for digital imaging



Nobel prize in physics 2009

George E. Smith & Willard S. Boyle

“for the invention of an imaging semiconductor circuit – the CCD sensor”

Original discovery made at AT&T Bell Labs in 1969

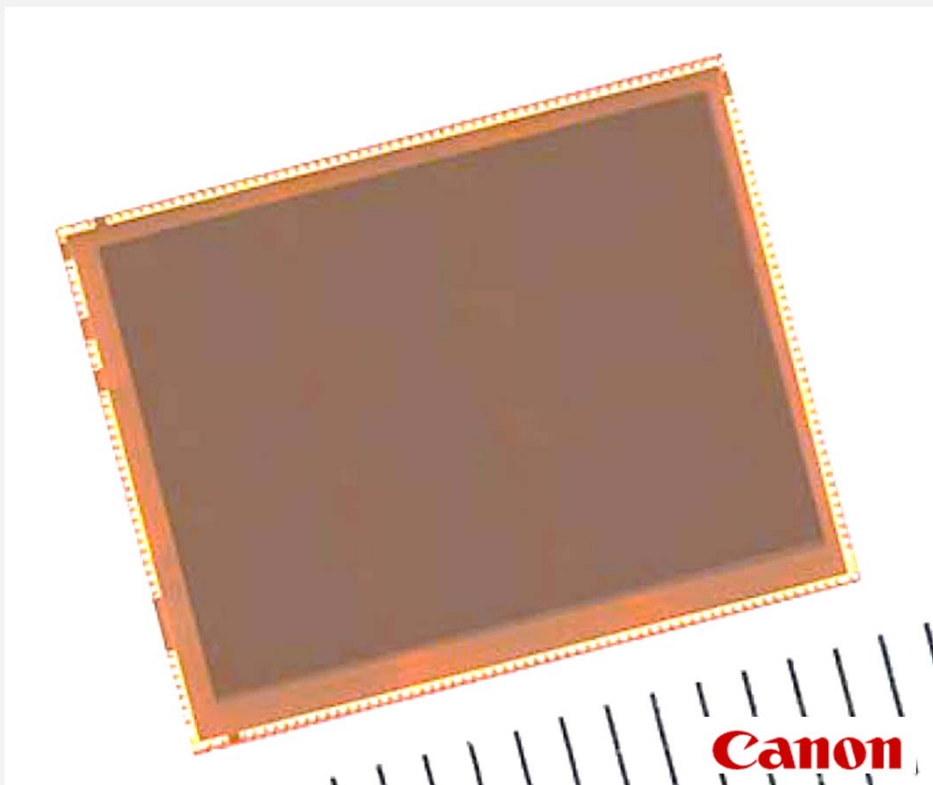
Toward the post-CCD era in spectroscopy

CCD limitations

No high time resolution

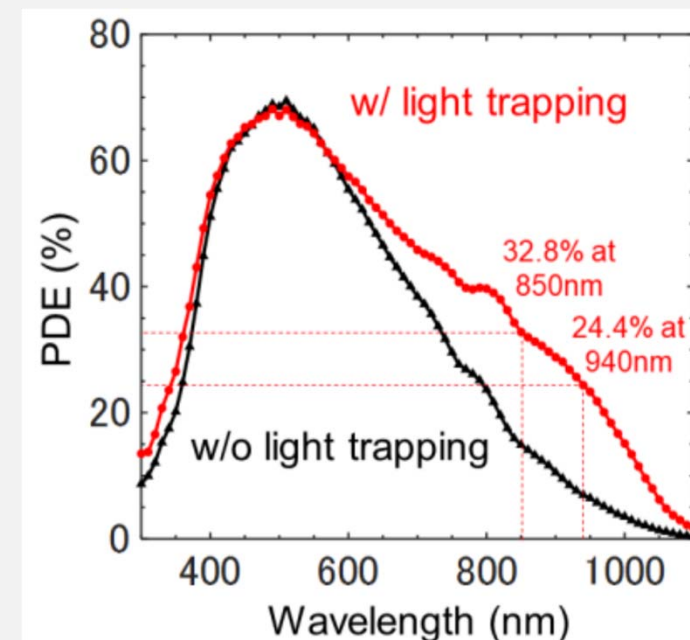
No photon counting

SPAD array (Single Photon Avalanche Diode)



Top tier
SPAD Pixel Array
2072(H) × 1548(V)
6.39 μ m-pitch

Bottom tier
Pixel Circuit Array
2072(H) × 1548(V)
6.39 μ m-pitch



13.2 mm × 9.9 mm² 3.2 Megapixel SPAD sensor array

Timing jitter 100 ps, zero read noise, maximum Photon Detection Efficiency 69%

Role of high time-resolution detectors

I. Remedy for anthropogenic effects

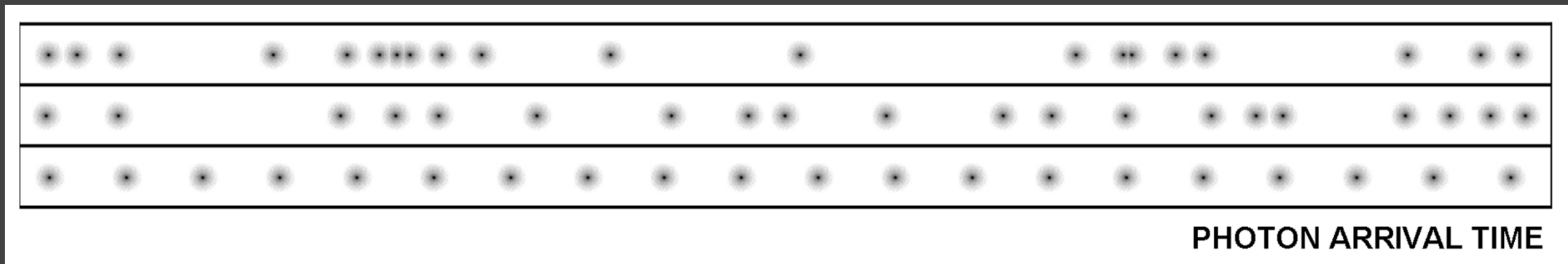
C2019 Y4 ATLAS

A night sky image featuring a dense grid of white satellite trails from Starlink, a bright comet (C2019 Y4 ATLAS) at the bottom left, and a blue meteor streak in the center.

Starlink satellite trails; Comet C2019/Y4 (ATLAS) at lower left. Image by Zdenek Bardon, <http://www.bardon.cz>

Role of high time-resolution detectors

II. Quantum-optical statistics of photon streams



Top: Bunched photons (Bose-Einstein; 'quantum-random')

Center: Antibunched photons (like fermions)

Bottom: Coherent and uniformly spaced (like ideal laser)

Toward the post-CCD era in spectroscopy

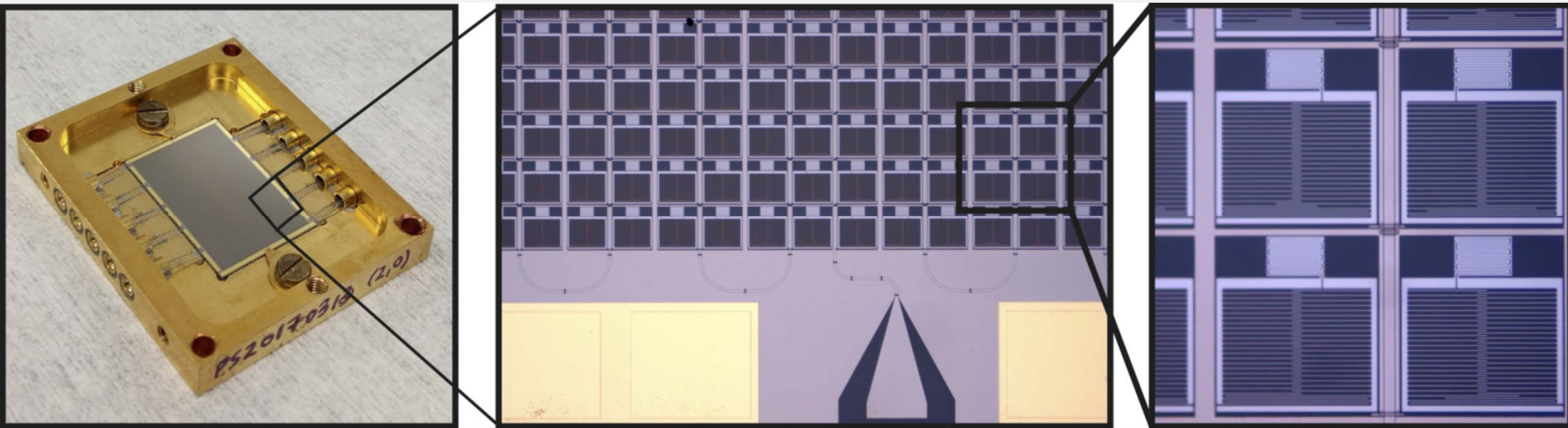
CCD limitations

No high time resolution

No photon counting

No energy resolution

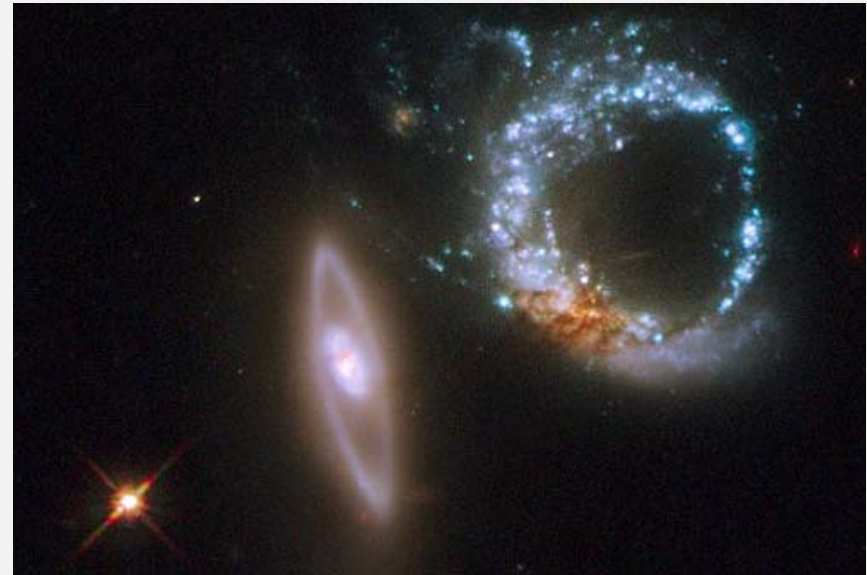
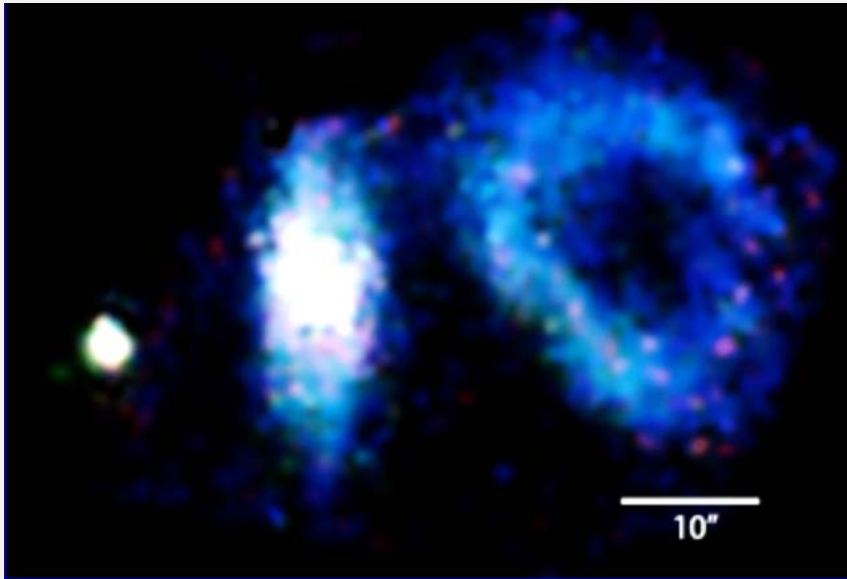
MKIDs, Microwave Kinetic Inductance Detectors



Left: 10,000-pixel MKID array for the DARKNESS instrument on Palomar 200" Hale telescope

Center & Right: Meandered patches are the photosensitive inductors, sparse sections are capacitors giving each MKID a unique resonant frequency. A microlens array boosts the effective fill factor to 90%.

MKIDs, Microwave Kinetic Inductance Detectors



Interacting pair of ring galaxies - Arp147

Left: With the MKID camera *ARCONS* at the Palomar 200" telescope. (Mazin lab, UCSB)

Right: With HST, assembled from three filters on WFPC2. (<http://hubblesite.org>)

But, wait...

**What information
is still missing?**

Toward the post-CCD era in spectroscopy

CCD limitations

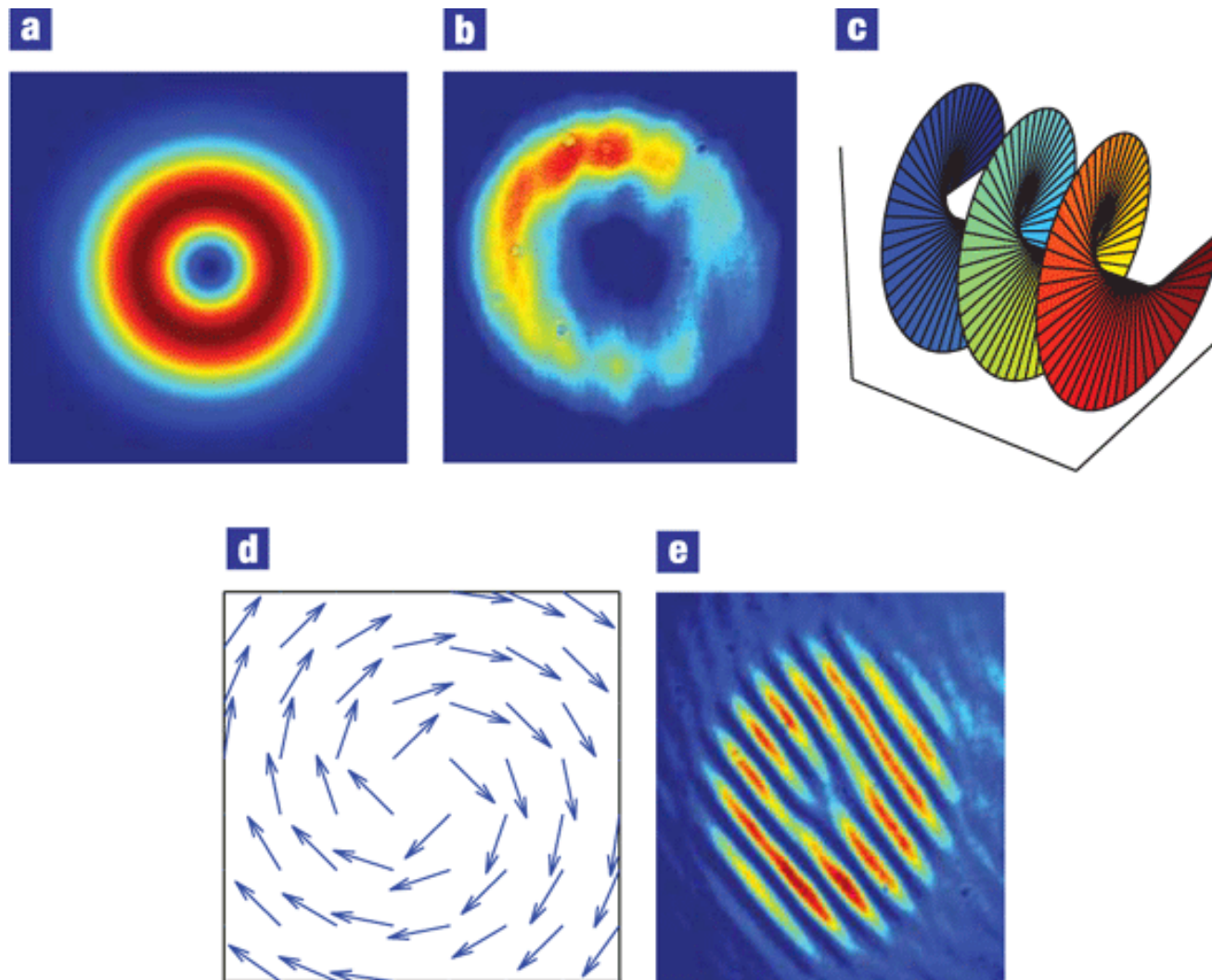
No high time resolution

No photon counting

No energy resolution

No polarization resolution

No photon orbital momentum

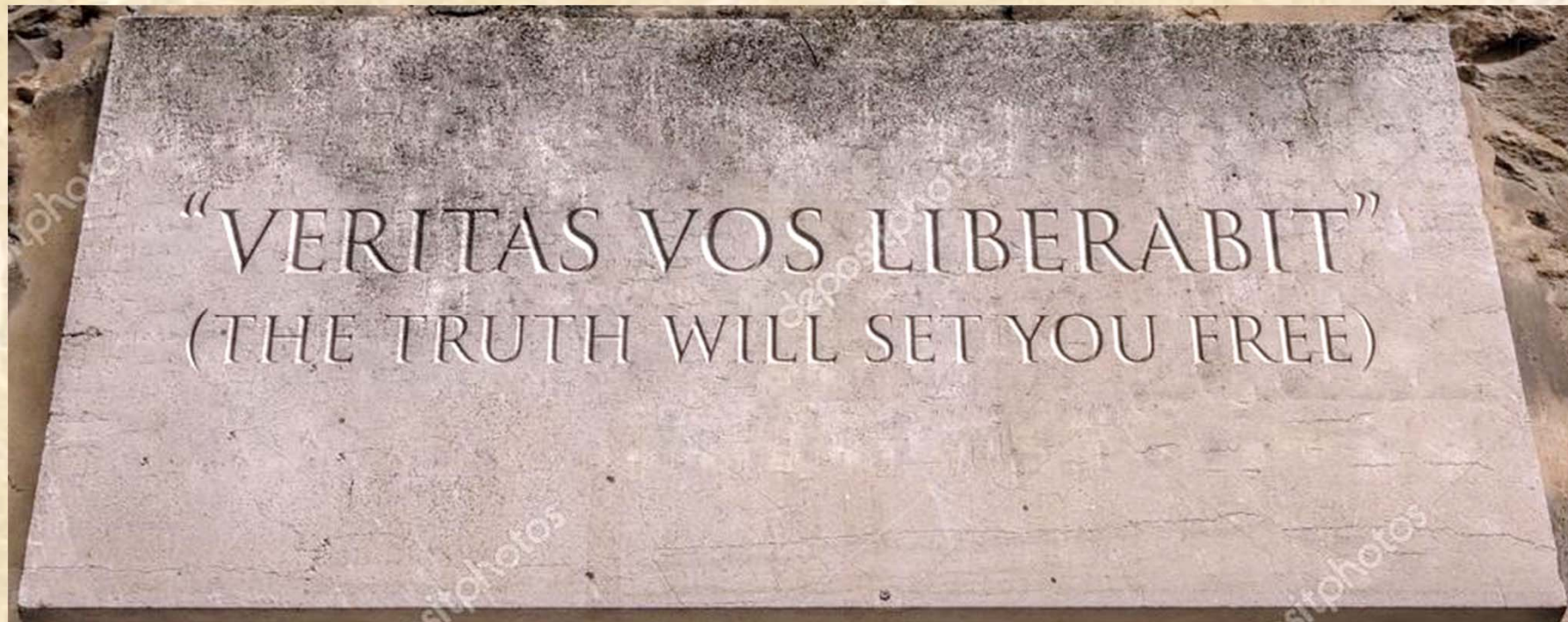


Light with photon orbital angular momentum

- Transverse intensity patterns of a light beam; **a**: theoretical; **b**: experimental
c: Phase twists around the central dark spot, producing a staircase-like phase wavefront
d: Local momentum mimics a tornado or vortex fluid – “optical vortices”
e: Interference pattern for $m = 1$, revealed by the fork-like structure.

Bottom line:

High-fidelity spectroscopy, combined with quantum optics, remains a challenge for ELT and beyond



THE
END